GENETIC INHIBITION OF THE UBIQUITIN-PROTEASOME PATHWAY: INSIGHTS INTO PROTEASOMAL TARGETING

Thesis by

Nazli Ghaboosi

In Partial Fulfillment of the Requirements for the Degree of

Doctor of Philosophy

CALIFORNIA INSTITUTE OF TECHNOLOGY

Pasadena, California

2007

(Defended April 4, 2007)

ACKNOWLEDGEMENTS

I would like to thank my adviser, Ray Deshaies, whose admirable expertise and devotion to research taught me how to think about science. Thank you to the Howard Hughes Medical Institute for funding my graduate work. My gratitude also goes to my colleagues in the Deshaies laboratory, particularly Rati Verma and Rob Oania for their patience in teaching me the details of yeast biology, especially the remarkable skill required to purify proteasome complexes from cells.

Thanks to my committee members Paul Sternberg, Bruce Hay, and Alex Varshavsky for their support throughout the years. When I first started this project, I turned to Alex Varshavsky for advice, as his own examination of an E1 mutant provided scientific breakthroughs that created an entire field of research. That initial conversation gave me invaluable insights into the problem I was tackling and more motivation than he knows. Over the years, I looked over my notes from that day more than once. Thank you to Bruce Hay and Paul Sternberg for personally taking the time to train me during my first clueless year of graduate school. Their passion for teaching is clear in their devotion to explaining complex genetics to someone who had never even seen *Drosophila* or *C. elegans* before.

Thanks to my wonderful, brilliant friends at Caltech, especially the ladies of girls' lunch; they made my time here enjoyable and allowed me to keep my sanity through all those late nights in lab.

I am deeply grateful to my family for their unwavering support and unconditional love. Thanks to my fiancé Fahim, who appeared in my life during the last year of my PhD when I was most in need of motivation. His passion for mathematics reignited my own intellectual curiosity at the most crucial time in my education. He gave me the courage to complete my final experiments with pleasure. I appreciate all of the love and support I received from him and his family as I undertook the arduous task of completing years of research.

My deep gratitude goes to my brother Reza, who was my roommate throughout most of the adventure of graduate school, and whose countless hours of reading law books made reading genetics papers seem fun in comparison. I could not have survived graduate school (or life) without his constant support and friendship. I would also like to especially thank my father Majid, whose passion for knowledge inspired me throughout my life, and who taught me everything I know, from literature to film to calculus.

Most of all, this thesis is dedicated to my mother, Nadereh Ansari. Her support, encouragement, and love have sustained me throughout my life. She cared so deeply for my education at every step, for which I am truly appreciative. Through her strength, wisdom, and grace, she has provided me with a model of how to be a successful scientist, and a successful human being. She is the inspiration behind the research involved in this thesis and behind everything that I achieve in life.

ABSTRACT

Regulated proteolysis plays a major role in diverse cellular processes, including cell-cycle progression, endocytosis, apoptosis, transcription, and signal transduction. Proteins destined for proteolysis undergo two key steps in the ubiquitin-proteasome pathway. First, a complex enzymatic cascade controls conjugation of a multiubiquitin chain onto a protein. Once ubiquitinated, protein substrates must be recognized and targeted to the proteasome complex, where they are unfolded and degraded. Receptor proteins, such as Rad23, recognize ubiquitinated proteins and deliver them to the proteasome.

While the list of enzymes involved in ubiquitination is steadily growing, the first enzymatic reaction required for all ubiquitin-dependent processes is catalyzed by one protein, the ubiquitin-activating enzyme, E1. In this work, we describe a genetic screen that targets the *Saccharomyces cerevisiae* E1 gene, *UBA1*. We report the isolation of *uba1-204*, a temperature-sensitive allele *UBA1* that exhibits dramatic inhibition of the ubiquitin-proteasome pathway. Shifting mutant cells to the restrictive temperature results in the depletion of cellular ubiquitin conjugates within minutes, accompanied by stabilization of multiple protein substrates. We have employed the tight phenotype of this mutant to investigate the role ubiquitin conjugates play the recognition and delivery of substrates to the proteasome.

It is possible to purify intact and active proteasomes complexes from *uba1-204* cells. In the absence of ubiquitin activation, these proteasome complexes are depleted of ubiquitin conjugates and the ubiquitin-binding receptor proteins Rad23 and Dsk2. Binding of Rad23 to these proteasomes *in vitro* is enhanced by addition of either free or substrate-linked ubiquitin chains. Moreover, association of Rad23 with proteasomes in mutant and wild-type cells is improved upon stabilizing ubiquitin conjugates with proteasome inhibitor. We propose that recognition of polyubiquitin chains by Rad23 promotes its shuttling to the proteasome *in vivo*. As an additional example of the value of this novel genetic mutant in the study of the ubiquitin-proteasome system, we present preliminary results from a quantitative mass spectrometric analysis of the proteins associated with proteasome complexes isolated from *uba1-204* cells.

In summary, we have created a genetic method of rapidly inhibiting the ubiquitin-proteasome system. This will enable future exploration of the ubiquitin-proteasome system and potentially many other ubiquitin-dependent cellular processes.

TABLE OF CONTENTS

LIST OF FIGURES

Chapter 1

BACKGROUND

THE DISCOVERY OF UBIQUITIN

Ubiquitin, a small 76 residue protein named for its ubiquitous presence ("probably represented universally in all living cells"), was first identified by Goldstein et al. in 1975. While its function remained a mystery, it was found to be part of a branched protein covalently linked to histone 2A (Goldknopf and Busch 1977). In 1980, ubiquitin was purified and found to ligate onto proteins in an ATP-dependent manner, and it was proposed that this ligation marked proteins for proteolysis (Hershko et al. 1980).

The discovery of ubiquitin and its conjugation onto proteins lead to dissection of the complex enzymatic cascade involved in regulating the ubiquitination process. The first reaction required for all ubiquitin-dependent cellular functions is the activation of ubiquitin by ubiquitin-activating enzyme, or E1 (Ciechanover et al. 1981). E1 activates ubiquitin by catalyzing a two-step process. First, the E1 enzyme forms a ubiquitin-adenylate intermediate in an ATP-dependent reaction. Ubiquitin is then transferred to an active-site cysteine residue of E1 to form a covalent thioester bond (Ciechanover et al. 1981). E1 can then transfer the activated ubiquitin moiety to a cysteine residue on a ubiquitin conjugating enzyme (E2) (Hershko et al. 1983; Pickart and Rose, 1985), and thereafter to a substrate with the help of a ubiquitin ligase protein (E3) (Hershko et al. 1983). A full historical account of early biochemical discoveries in the ubiquitin-proteasome system can be found

in Finley, Ciechanover, and Varshavsky (2004), Hershko et al. (2000), and Ciechanover (2005).

A major genetic breakthrough came in 1984, when Varshavsky and colleagues characterized a temperature-sensitive mouse cell line with a defect in proteolysis and showed for the first time that ubiquitin conjugation and protein degradation are linked *in vivo* (Ciechanover et al. 1984; Finley et al. 1984). This cell line (ts85) was shown to carry a conditional allele of the ubiquitin-activating enzyme, E1. This work demonstrated that ubiquitin conjugation is required for proteolysis, cell viability, cell-cycle progression, and stress response, revealing the scope of ubiquitination in mammalian cells.

Further work went on to define the first degradation signals and identify some of the enzymes involved in the pathway. It is now appreciated that regulated proteolysis is responsible for controlling a broad array of cellular processes, including cell-cycle progression, endocytosis, apoptosis, transcription, antigen presentation, signal transduction, and protein quality control. The significance of the ubiquitin-proteasome system was acknowledged in 2004 when the Nobel Prize in Chemistry was awarded "for the discovery of ubiquitin-mediated protein degradation."

THE UBIQUITIN-PROTEASOME SYSTEM

The ubiquitin-proteasome system is involved in many cellular processes including differentiation, cell-cycle control, and DNA repair. Two key steps are required for regulated proteolysis: covalent attachment of a polyubiquitin chain onto the target substrate and delivery of ubiquitinated substrates to the proteasome complex for degradation.

Ubiquitination involves a complex enzymatic cascade that controls protein conjugation with ubiquitin. This results in an isopeptide bond with lysine residues on the target substrate and, subsequently, with another ubiquitin to extend the ubiquitin chain. Once ubiquitinated, protein substrates must be recognized and targeted to the proteasome complex, where they are unfolded and degraded. The 26S proteasome is an ATP-dependent multisubunit complex composed of a barrel-like 20S core complex flanked by one or two 19S regulatory complexes. The 19S cap is thought to mediate recognition of ubiquitin-protein conjugates, catalysis of isopeptidase reactions to remove the polyubiquitin chain, and denaturation of the protein. The substrate is then transported through the central channel where it is degraded at the active site by endopeptidases to produce short polypeptides.

The first enzyme in the ubiquitin-proteasome pathway, E1 ubiquitin-activating enzyme, is encoded in *Saccharomyces cerevisiae* by the essential gene *UBA1* (McGrath et al. 1991) and is required to catalyze the first step in all ubiquitin-mediated processes. A single budding yeast E1 protein, Uba1, is responsible for initiating the intricate downstream ubiquitination network consisting of 11 E2s and 54 potential E3s that act on a multitude of proteins, marking them for destruction. The increasing complexity of this pathway is regulated by increasing specificity of recognition between E2s and E3s, and then with these enzymes and the many varied protein substrates. Once these substrates are polyubiquitinated however, the complex pathway again tapers to one end – the 26S proteasome—where the ubiquitinated substrates are recognized and broken down.

The ubiquitin-proteasome pathway was originally thought to culminate in a stochastic interaction between polyubiquitin chains and the proteasome. However, the selective recognition of ubiquitinated proteins is emerging as a key regulatory step in

proteolysis. Protein recognition and targeting mechanisms must also be highly regulated in order to avoid indiscrimate degradation. We have only begun to understand the complex mechanisms involved in targeting ubiquitinated proteins to the proteasome. Multiubiquitin chains bind Rpn10, a subunit of the 19S regulatory complex. In addition to Rpn10, it has recently been shown that several proteasome-interacting proteins, including Rad23 and Dsk2, act as ubiquitin receptors in order to confer yet another level of substrate selectivity. These proteins act as adaptors, associating with the proteasome via ubiquitin-like domains (UbL) and recognizing ubiquitin chains via ubiquitin-associated domains (UBA). One of the outstanding questions regarding the mechanistic details involved in substrate delivery is whether UbL/UBA proteins remain docked on the proteasome, awaiting ubiquitinated proteins, or first bind to ubiquitinated proteins and function to deliver them to proteasome complexes.

RESEARCH OBJECTIVES

The initial goal of this thesis was to create a rapid, powerful method for shutting down the ubiquitin-proteasome system in *Saccharomyces cerevisiae*. This powerful tool would enable us to use a global approach to exploring unanswered questions regarding the regulation of the ubiquitin-proteasome system. In the subsequent chapters of this thesis, I describe the generation of a new genetic mutant strain of *S. cerevisiae* and offer examples of how this strain can provide a unique perspective with which to better understand ubiquitin-dependent cellular processes.

In chapter 2, I discuss in detail the genetic screen in which we created temperature-sensitive alleles of the essential ubiquitin-activating enzyme, *UBA1*, and

review initial phenotypic characterization of mutant alleles. From this screen, *uba1-204* emerged as the first strong loss-of-function allele of the *S. cerevisiae UBA1* gene.

Chapter 3 was published as an article entitled "A conditional yeast E1 mutant blocks the ubiquitin-proteasome pathway and reveals a role for ubiquitin conjugates in targeting Rad23 to the proteasome" on March 14, 2007 in *Molecular Biology of the Cell*. Here, I discuss in further detail the full characterization of the conditional phenotype observed in *uba1-204* cells. Within five minutes of shifting mutant cells to the restrictive temperature, all detectable ubiquitin conjugates are lost. Mutant cells exhibit a cell-cycle arrest phenotype and a defect in the proteolysis of several ubiquitin-proteasome pathway substrates. These results establish *uba1-204* cells as a rapid method of inhibiting the ubiquitin-proteasome pathway. In analyzing the cellular effects of such a severe genetic assault, we observed that, while 26S proteasome complexes appeared structurally intact, they exhibited changes in their association with ubiquitin-binding receptor proteins, such as Rad23. We conclude this chapter by exploring the significance of our observation that Uba1 activity is required for efficient targeting of ubiquitin-binding proteins to the proteasome. Thus, we are able to exploit the unique ubiquitin chain-free cellular environment in the mutant strain to answer a question about the mechanism of ubiquitin receptor targeting *in vivo* that could not be easily addressed any other way.

In chapter 4, I describe the results from a preliminary quantitative mass spectrometric analysis of proteasome complexes isolated from *uba1-204* cells. MudPIT, or multidimensional protein identification technology, allows identification and quantitation of proteins in a complex peptide mixture. By coupling this powerful proteomic technique to the method of affinity-purifying intact proteasome complexes from yeast cells, it is possible to examine the impact of blocking the ubiquitin-proteasome pathway on the association of

proteins with the proteasome. While this work is incomplete without validation of some of our results, it is included as further proof of the value of the *uba1-204* tool described here to gain unique insight into the ubiquitin-proteasome system.

Chapter 2

SCREEN FOR TEMPERATURE-SENSITIVE ALLELES OF *S. CEREVISIAE UBA1*

INTRODUCTION

The 3075 base pair *Saccharomyces cerevisiae* ubiquitin-activating enzyme gene, *UBA1,* encodes a 1024 residue protein that is highly conserved throughout evolution (Figure 2-1). There are two active sites on the E1 protein, the adenylation site and the active-site cysteine. This drives the two-step enzymatic process in which two ubiquitin moieties can be bound simultaneously, with one forming an adenlyate intermediate while the other is transferred to the thiol site (Figure 2-2).

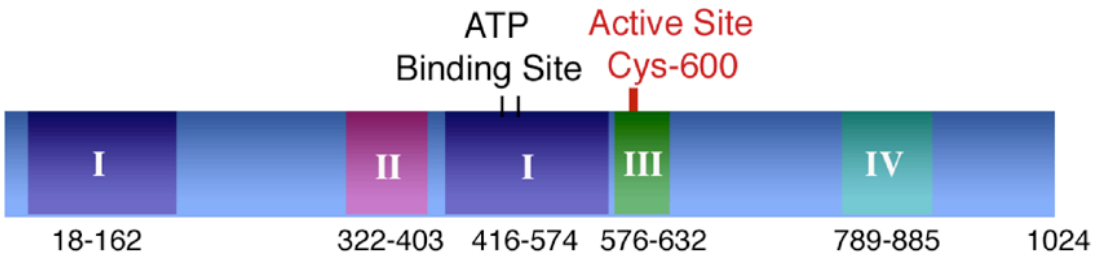

Figure 2-1. Schematic representation of the *S. cerevisiae* E1 protein, Uba1. Uba1 contains 1024 residues with four conserved domains. Domain I contains the nucleotide-binding motif and is found in many proteins, including those not involved in the ubiquitin pathway. Domain III contains the active-site cysteine

residue. Domains II and IV are found in several proteins but their function is not known (Hochstrasser, 1998). Residues included in each domain are specified.

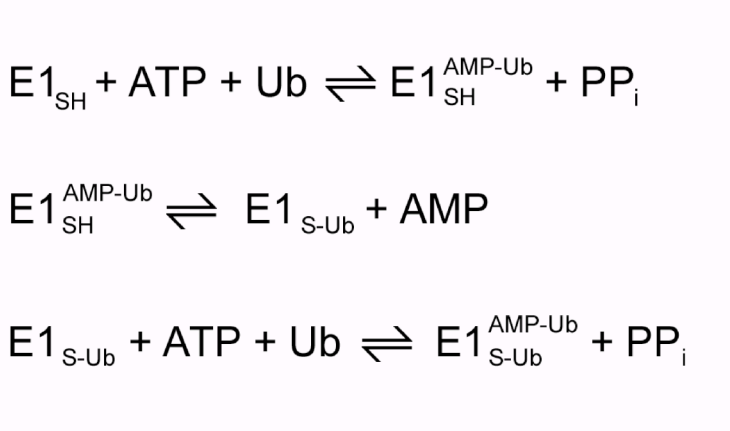

Figure 2-2. Activation of ubiquitin by E1. E1 first interacts with ATP and ubiquitin to form a ubiquityl-AMP intermediate at its ATP binding site. In a second reaction, the ubiquitin moiety is transferred to the E1 active-site cysteine residue to create a high-energy thioester linkage.

The activation of ubiquitin and, therefore, all ubiquitin-dependent processes requires one key protein, E1. Poised at the apex of the pathway, this protein provides a unique means of perturbing the entire downstream ubiquitin system. Mutant alleles of E1 have been instrumental in dissecting the functional significance of many aspects of the ubiquitin-proteasome system. The first thermolabile E1 mutant was encountered in the ts85 derivative of the FM3A spontaneous mouse mammary carcinoma cell line (Finley et al. 1984). These cells arrested in early G2 and late S phase and failed to degrade short-lived proteins *in vivo* (Ciechanover et al. 1984). Another mammalian E1 mutant, E36-ts20, was later identified in hamster lung fibroblast cells (Kulka et al. 1988). This mutant

displayed similar defects in ubiquitin-protein conjugation and degradation of short-lived proteins. Interestingly, these mutant cells also arrested at late S/early G2 phase. A third E1 mutant, A31N-ts20, was found in Balb/c 3T3 mouse embryo fibroblast cells that had been subjected to chemical mutagenesis (Salvat et al. 2000). Again, a defect was observed in the degradation of specific proteins, but like other mammalian mutants, a leaky E1 inactivation phenotype suggested that the E1 reaction is not rate-limiting in ubiquitination (Salvat et al. 2000).

While examination of mammalian E1 mutants yielded valuable insights into the ubiquitin-proteasome system, there has been little work to characterize a strong allele of *S. cerevisiae* E1 enzyme since the first mutant alleles were described alongside original experiments to clone the gene (McGrath et al. 1991). All yeast *uba1* alleles that have been described previously are hypomorphic alleles that achieve only partial inactivation of the pathway. In McGrath's dissertation (1991), he described isolating three mutants of *uba1*, including *uba1-26*. *Uba1-26* is currently the most widely used mutant *uba1* strain, often examined as a control in experiments studying various aspects of the ubiquitin-proteasome system. However, in initial experiments to determine the scope of its proteolytic defect, it was found that "the turnover of naturally short-lived proteins labeled during a 5 minute pulse…was unaffected in the *ts26* mutant" (McGrath, 1991), indicating that the temperature sensitivity was not due to extensive protein stabilization. In addition, these mutants were never well characterized, and the affect on ubiquitination was not examined. Despite their leaky E1 inactivation phenotype, these mutant cells have proven useful in many studies of ubiquitin-dependent processes. Palanimurugan et al. (2004) used *uba1-2*6 with other ubiquitin pathway mutants to establish the ubiquitin-dependent degradation of Oaz1. Gandre and Kahana (2002) observed moderate stabilization of Ub-

R-LacZ. While the observed protein stabilization was a sufficient control to establish the ubiquitin dependence of the turnover of these specific proteins, it is doubtful that this mutant would be useful for broader shutdown of the ubiquitin-proteasome system.

Meanwhile, the *uba1-2* allele was isolated in a screen for defects in Deg1-βgal degradation and was caused by a transposon insertion upstream of the coding sequence, resulting in reduction of wild-type Uba1 protein expression. This allele results in only ~3-fold stabilization of Leu-βgal, Ub-Pro-β gal, and Ste3, and only "modest stabilization" of short-lived proteins α2 and a1 (Swanson and Hochstrasser 2001). Finally, other alleles were subsequently isolated as suppressors for various genetic mutations (*uba1-165* suppressed *mcm3-10* in Cheng et al. 2002; *uba1-o1* suppressed *orc2-1* in Shimada et al. 2002), but their mutant phenotypes are defined only in the context of their respective screens.

The limitations of existing *uba1* alleles motivated our initial screen to isolate a strong loss-of-function *uba1* allele. This is the first direct screen to isolate a conditional yeast E1 gene since the gene was first cloned in 1991 (McGrath et al. 1991). Whereas most other mutants had been isolated in screens for various genetic pathways, which were not directly related to the ubiquitin-proteasome system, we employ a more direct "reverse genetic" approach. By directly mutagenizing the gene of interest, a large population of potential conditional alleles is generated. Furthermore, the method of error-prone PCR mutagenesis described can yield a wide spectrum of mutant phenotypes that had not been created before. Whereas earlier hypomorphic alleles have proven useful in confirming the ubiquitin dependence of the turnover of specific proteins, they highlight the potential value of a stronger conditional allele with broad utility in exploring the entire ubiquitin conjugation

pathway. Among the many issues that could be addressed with a tight and rapid-acting temperature-sensitive mutation in *UBA1* is the question of how ubiquitin conjugates contribute to the proteasomal targeting of substrates destined for proteolysis.

RESULTS

Generation of mutant alleles of UBA1 by random PCR mutagenesis

Error-prone PCR was performed using the Genemorph II Random Mutagenesis Kit (Stratagene, La Jolla, CA) according to protocols listed in the product specifications, using a target DNA amount ranging from <0.1 to 1000 ng in order to produce a wide range of mutation frequencies. A large amount of target DNA (500-1000 ng) is recommended to achieve a low mutation frequency (0-4.5 mutations/kb), while using a lower amount of target DNA (0.1-100 ng) results in higher mutation rates (>9 mutations/kb). The mutant *uba1* gene products from the various PCR reactions were pooled and co-transformed into RJD3268 cells, along with pRS313 plasmid that had been linearized with *NheI*. It is notable that the mutant strain isolated in this screen, *uba1-204*, was the result of a mutation rate of 4.5 mutations/kb (Figure 2-12).

Genetic screen for temperature-sensitive phenotype

A plasmid shuffling strategy was used to isolate cells that contained a genomic deletion of the essential UBA1 gene and carried only a mutant copy of the gene. The entire coding region at one locus in a diploid W303 wild-type yeast strain was replaced

with the KanMX marker. Gene disruption was verified by PCR and by sporulation and tetrad dissection. The resulting strain, RJD3267 also contained a partial deletion of the overlapping Ste6 gene, causing sterility in mating type a cells. Mutant plasmids were introduced into uba1Δ haploid cells sustained by a low copy URA3 plasmid containing UBA1. Transformants were plated on 5-fluoro-orotic acid (5-FOA) to evict the UBA1 plasmid and clones sustained by the mutagenized plasmid were sought (Figure 2-3). Plates were replica plated onto YPD plates and stored at 37°C to score for temperature sensitivity (Figure 2-3).

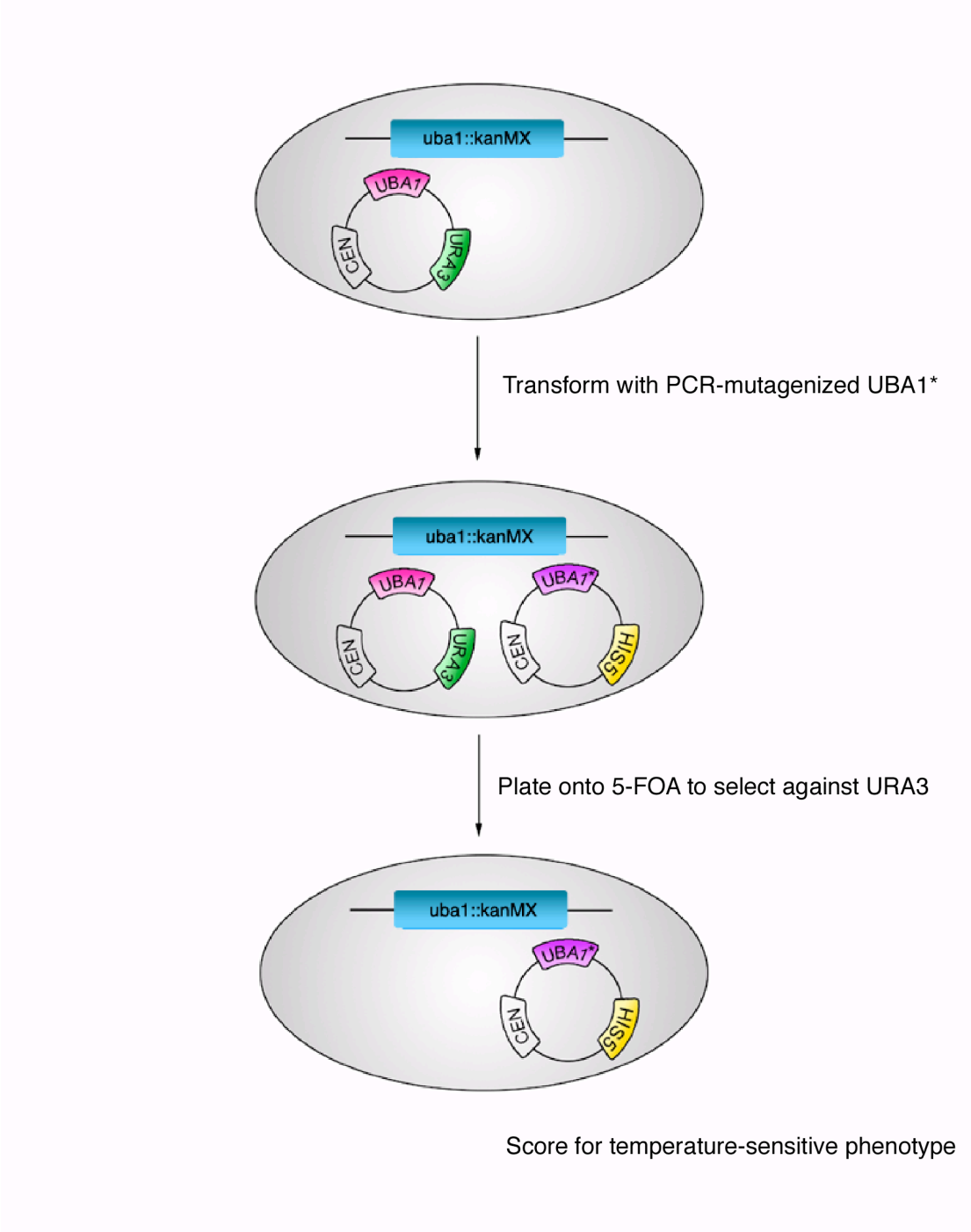

Figure 2-3. Schematic of the plasmid shuffling strategy employed to isolate mutant alleles of UBA1. The gene was deleted in diploid W303 cells by PCR

and replaced with the Kanmx marker. Wild-type UBA1 was introduced into cells on the pRS316 URA3 plasmid. Cells were sporulated and a haploid clone was isolated. The strain was then transformed with PCR-mutagenized UBA1 and a linearized HIS5 plasmid that contained regions of homology to the PCR product. Transformants were replica plated onto 5-FOA plates to identify clones, which had lost the URA3 plasmid. Plates were replica plated onto YPD plates and stored at 37°C to score for temperature sensitivity.

After selecting for replacement of the URA plasmid with the HIS plasmid harboring the mutagenized PCR product, colonies were replica plated onto duplicate YPD plates and incubated at 25°C and 37°C (Figure 2-4). We identified fifty clones which grew at 25°C but not at 37°C.

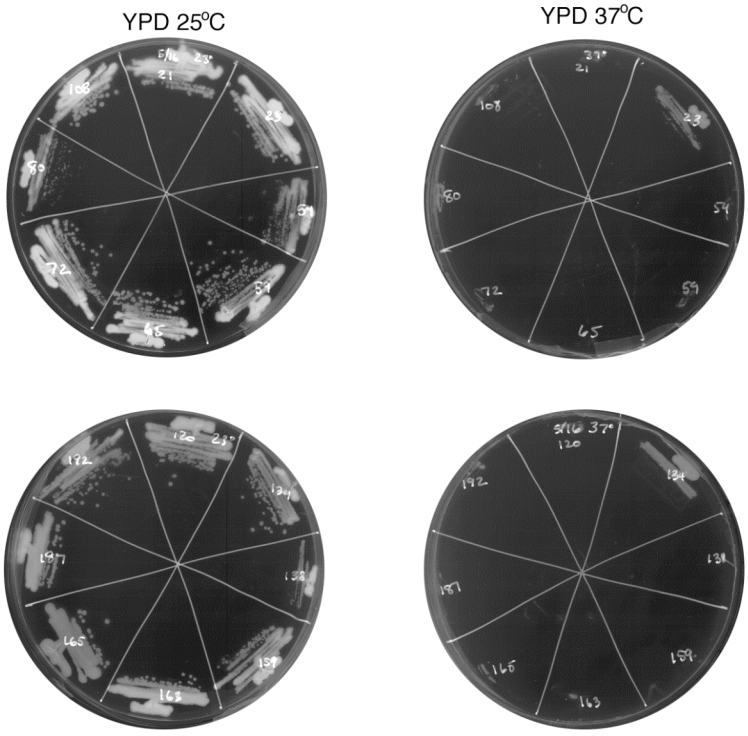

Figure 2-4. Sample of temperature-sensitive *uba1* mutants. Strains were plated onto YPD and incubated at 25°C and 37°C to verify temperature-sensitive phenotype of isolated clones.

Considering the failure of most E1 mutant alleles isolated in mammalian cells and in yeast to produce a discernable effect on bulk ubiquitin conjugation, we did not test directly for ubiquitination defects. However, these previously characterized E1 mutants were found to stabilize specific proteins (Salvat et al. 2000; Palanimurugan et al. 2004). *Uba1* mutants were tested for stabilization of a well-characterized short-lived substrate of the ubiquitin-proteasome pathway, Ub^{V76}-V-βgal (Johnson et al. 1995). Ub^{V76}-V-βgal is a

ubiquitin-βgalactosidase fusion protein in which the carboxy-terminal glycine residue of ubiquitin is mutated to a valine residue. This mutation blocks ubiquitin cleavage, rendering the fusion protein unstable *in vivo*. The "non-removable" N-terminal ubiquitin fusion protein is targeted for degradation by the UFD (Ubiquitin Fusion Degradation) pathway (Johnson et al. 1995). An initial test of protein stabilization was conducted using wild-type and mutant cells expressing Ub^{V76}-V-βgal under control of the *GAL1* promoter. Of the fifty isolated clones, most showed little stabilization of the substrate protein at the nonpermissive temperature (Figure 2-5, *ts93* and *ts211*). However, this initial screen for proteolytic defects lead us for focus on four clones for further analysis*: ts60*, *ts108*, *ts126* (Figure 2-5), and *ts204* (also referred to as *uba1-204*).

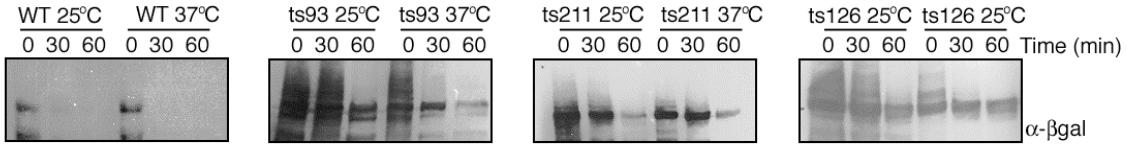

Figure 2-5. Sample of initial Ub^{V76}-V-βgal substrate stabilization experiment. Wild-type and mutant cells expressing Ub^{V76}-V-βgal under control of the *GAL1* promoter were grown in SD medium with raffinose and protein expression was induced by addition of 2% galactose for 1 hour. Cultures were then incubated at either 25°C or shifted to 37°C for 1 hour and transferred to dextrose medium pre-equilibrated at the same temperature to initiate a chase. Samples were withdrawn at indicated time points, lysed, separated by SDS-PAGE, and immunoblotted with antiserum to β-gal.

Characterization of four temperature-sensitive alleles of UBA1

Repeating the analysis of the turnover of Ub^{V76}-V-βgal in the four isolated *uba1* mutants verified that the substrate is degraded at permissive temperature but stabilized at the nonpermissive temperature (Figure 2-6). Cell growth was tested, and all four mutant alleles remained viable at 30°C and were completely inviable at 37°C (Figure 2-7). In addition, in all four mutant strains, cellular division ceased within one cell cycle of shifting cells to nonpermissive temperature (Figure 2-8).

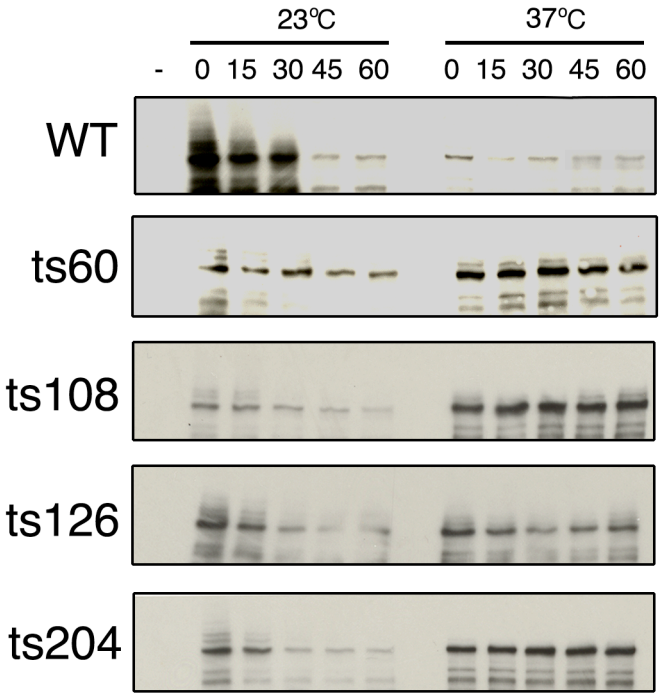

Figure 2-6. Four temperature-sensitive alleles of *uba1* stabilize Ub^{V76}-V-βgal, at the nonpermissive temperature. Wild-type and mutant cells expressing Ub^{V76}-V-βgal under control of the *GAL1* promoter were grown in SD medium with raffinose and protein expression was induced by addition of 2% galactose for 1

hour. Cultures were then incubated at either 25°C or shifted to 37°C for 1 hour and transferred to dextrose medium pre-equilibrated at the same temperature to initiate a chase. Samples were withdrawn every fifteen minutes for analysis. Lysates were separated by SDS-PAGE and immunoblotted with antiserum to β-gal. Control (-) sample was an isogenic strain lacking the plasmid.

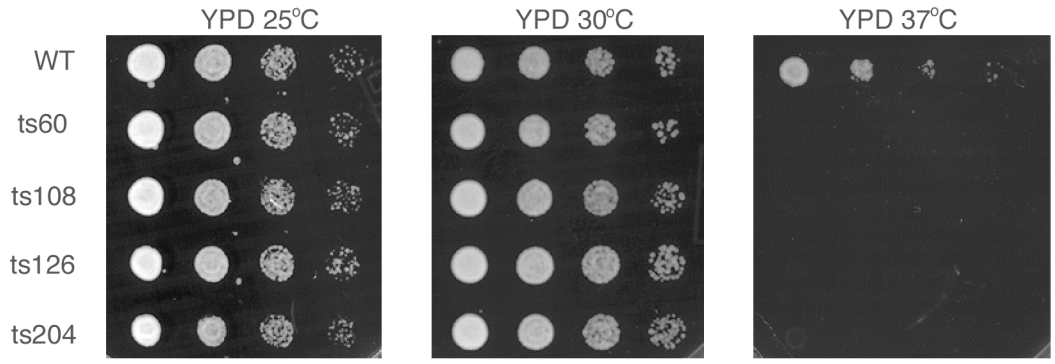

Figure 2-7. Growth defect at 37°C. Four temperature-sensitive alleles of *uba1* grow at 25°C and 30°C but failed to grow at the nonpermissive temperature, 37°C.

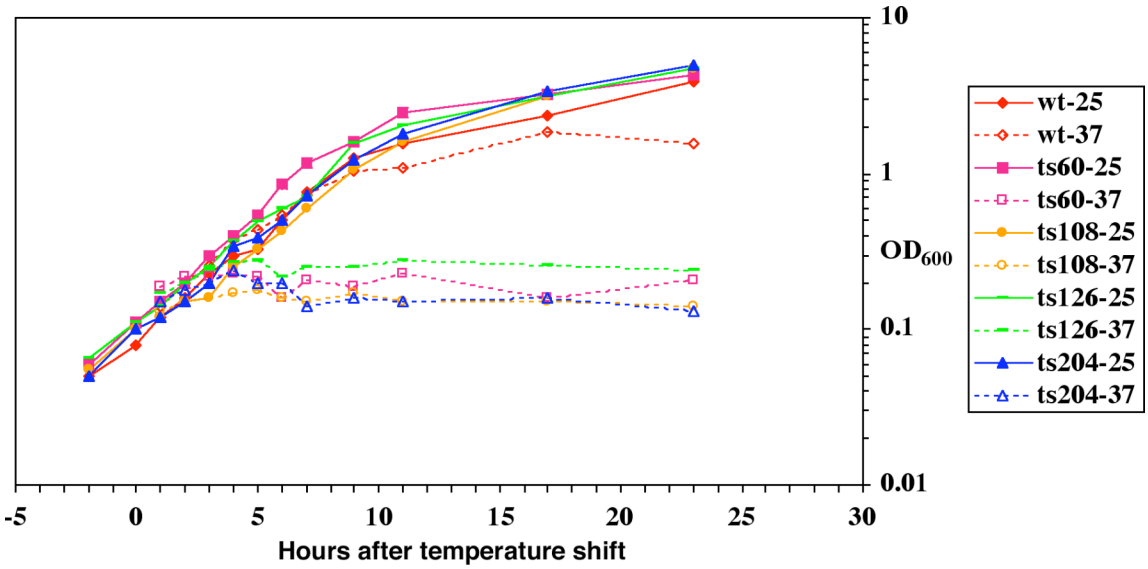

Figure 2-8. Cell growth in YPD medium measured by optical density. Mutant cells' growth is similar to wild-type at 25°C but in all four mutants, cellular division ceased within one cell cycle of shifting cells to 37°C.

In order to ascertain whether the proteolytic defect observed in *uba1* mutants would extend to other E2/E3 degradation pathways, the turnover of Deg1-GFP was analyzed. The Deg1 degradation signal found in the N-terminus of the yeast α2 repressor marks this protein for rapid degradation *in vivo* by the ubiquitin ligase Doa10 (Swanson et al. 2001). The turnover of this protein after a cycloheximide chase was followed and three mutants, *ts108, ts126*, and *ts204* displayed stabilization of the protein at 37°C (Figure 2-9).

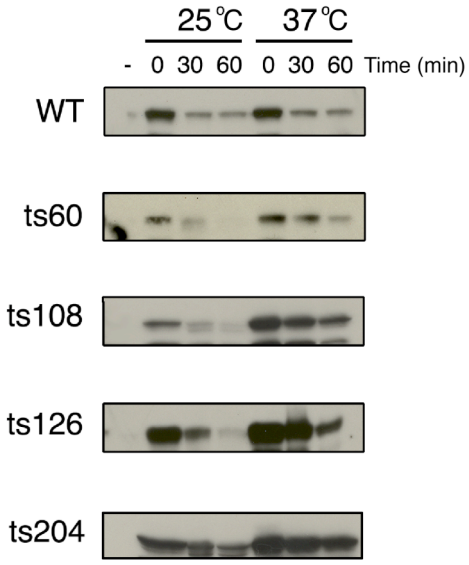

Figure 2-9. Stabilization of Deg1-GFP substrate. Wild-type and *uba1-204* cells expressing Deg1-GFP were grown in SD medium. Cultures of exponentially growing cells were incubated at 25°C or shifted to 37°C for 1 hour and cycloheximide was added to initiate a chase period. Samples were withdrawn every thirty minutes for analysis. Lysates were separated by SDS-PAGE and immunoblotted with antiserum to GFP. Control (-) sample was an isogenic strain lacking the plasmid.

The four mutant alleles were then tested for an effect on the amount of high molecular-weight ubiquitin conjugates present in cells within three hours of shifting the cells to the nonpermissive temperature. In lysates isolated from three of the alleles (*ts60*, *ts108*, and *ts126*), there was no discernable change in the amount of ubiquitin conjugates (Figure 2-10). This result was expected, as earlier E1 mutants showed a similarly weak inhibition of bulk ubiquitination. Surprisingly, lysates purified from *ts204* (hereafter referred to as *uba1-204*) cells seemed to be completely lacking all detectable ubiquitin conjugates

within one hour of incubation at 37°C (Figure 2-10). The experiment was repeated, analyzing samples each minute after the shift to nonpermissive temperature. Amazingly, in *uba1-204* cells, ubiquitin conjugates disappeared within five minutes of the temperature shift (Figure 3-2). This dramatic result lead us to focus our efforts on this exceptionally strong mutant allele *UBA1*.

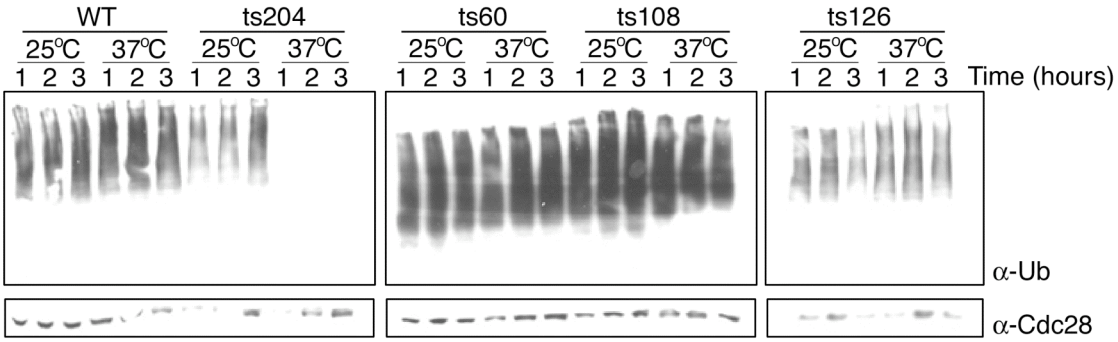

Figure 2-10. Loss of ubiquitin conjugates at the nonpermissive temperature in *uba1-204* cells. Wild-type and mutant *uba1* cells were grown to log phase in liquid YPD medium at 25°C. Half of each culture was shifted to the nonpermissive temperature and samples were withdrawn at indicated time points. Lysates were prepared and analyzed by SDS-PAGE and immunoblotted with antiserum to ubiquitin.

Characterization of uba1-204, a loss-of-function allele of UBA1

Most cells containing mutations in the ubiquitin pathway exhibit some type of cell-cycle arrest. While the two mammalian E1 mutants (*ts20* and *ts85*), derived from different

cell lines, both arrest at S/G2 boundary at restrictive temperatures (Ciechanover et al. 1984; Finley et al. 1984; Kulka et al. 1988). However, most yeast E1 mutants isolated thus far do not display a cell-cycle phenotype (McGrath, 1991; Swanson and Hochstrasser 2000). Only the cold-sensitive *uba1-165* mutant has a cell-cycle phenotype, arresting in G1 (Cheng et al. 2002). We postulated that the lack of cell-cycle arrest phenotypes observed in previously isolated yeast mutants could be due to their relatively mild phenotypes. Therefore, we expected that the relatively severe ubiquitination defect observed in *uba1-204* cells would be reflected in a defect in cell-cycle progression. However, microscopic analysis failed to reveal a clear cell-cycle arrest terminal phenotype (data not shown), although cellular division had ceased within one cell-cycle of shifting cells to the nonpermissive temperature (Figure 2-8).

To more closely examine the effect of *uba1-204* mutations on cell-cycle regulation, cellular DNA content was analyzed by flow cytometry. Intriguingly, it seemed that while wild-type cells continued their progression through the cell-cycle at 37°C, mutant cells arrested with some cells remaining in G1 and some in G2 (Figure 2-11). In later experiments discussed in chapter 3, our data reveal that *uba1-204* cells can arrest both in G1 and in G2. By synchronizing cells with alpha-factor and shifting them to the nonpermissive temperature during G1, we were able to demonstrate a G1 arrest phenotype (Figure 3-1C). Similarly, when cells were allowed to progress through the cell-cycle before shifting to 37°C, cells exhibited a G2 arrest phenotype (Figure 3-1D).

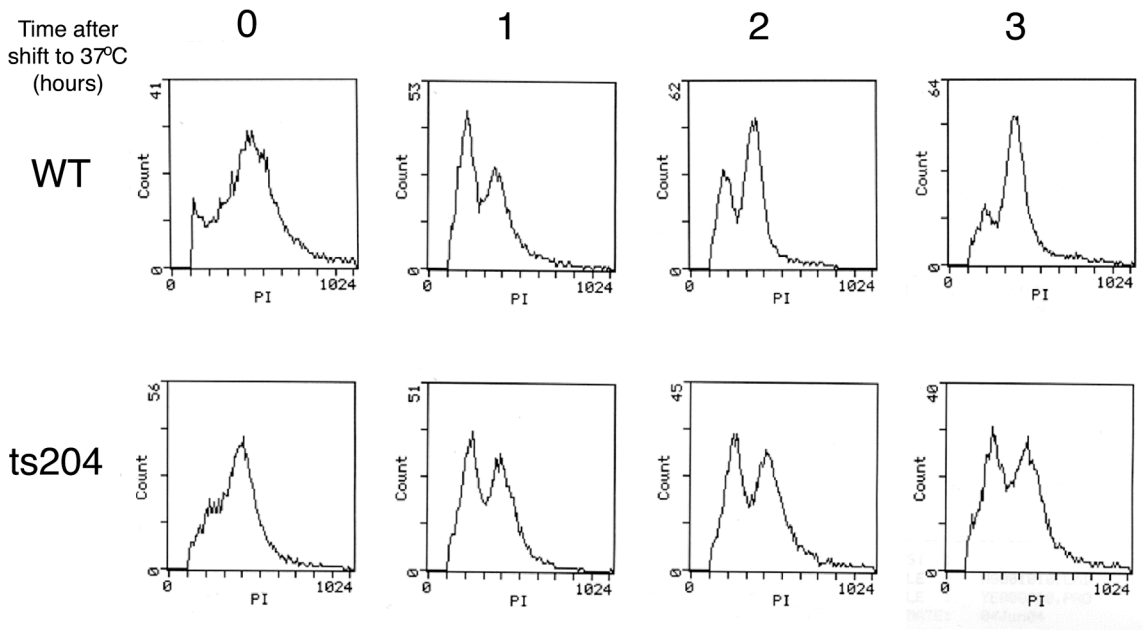

Figure 2-11. Cell-cycle arrest. Unsynchronized wild-type and *uba1-204* cells were grown to log phase at 25°C in YPD medium and shifted to 37°C at time 0. At indicated time points following the temperature shift, aliquots were withdrawn and prepared for assessment of total DNA content by fluorescence-activated cell sorting (FACS).

The viability of the mutant *uba1-204* strain at the nonpermissive temperature was tested. The number of colony forming units (CFU) per microliter in cultures of wild-type and *uba1-204* cells was determined at various times after the shift to 37°C by plating cells on YPD and counting colonies after two days of growth at 25°C. *Uba1-204* cells remain viable for up to an hour at the nonpermissive temperature after which there is a rapid loss of cell viability (Figure 2-12). Indeed, it was later discovered that when *uba1-204* cells incubated at 37°C for an hour are returned to 25°C, ubiquitin conjugates rapidly reappear (Figure 3-2B).

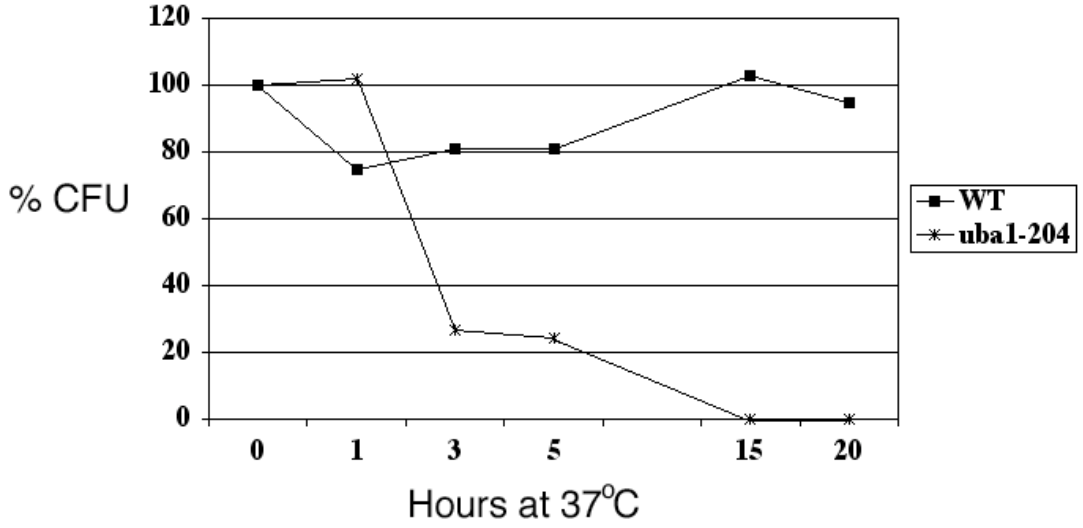

Figure 2-12. Cell viability. Cells were inoculated at low density in YPD medium and grown to log phase. At time 0, cultures were shifted to 37°C, and at indicated time points, samples were withdrawn and serially diluted. Five microliters of each dilution was plated onto YPD plates and incubated at 25°C for 2-3 days. The colony-forming units per microliter (CFU) were determined. Values represent percent CFU relative to time point 0 (25°C).

Sequence analysis

The mutant gene was sequenced and found to carry a total of fourteen mutations in its 3075 base coding sequence. This is equivalent to a mutation frequency of 4.6 mutations/kb. Six of the mutations were silent and the remaining mutations resulted in

eight amino acid changes to the 1024 residue protein: D318G, K401E, V502A, E523G, E534G, N630G, F680S, D936E.

Figure 2-13. Protein sequence of Uba1-204. Residues of the adenylation site, active site, and phosphorylation site are underlined. Eight amino acid changes identified in mutant protein are listed below the sequence.

The DNA of the other three isolated temperature-sensitive mutant genes was also sequenced in order to uncover any identical mutations or mutational “hot spots” which might provide a clue about key residues required for enzymatic activity (data not shown). However, none of the three mutant genes carried a mutation affecting the eight residues implicated in the conditional phenotype found in *uba1-204*.

DISCUSSION

In generating a strong loss-of-function allele of yeast E1, we reflected on the reasons that such a mutant had not been previously isolated, despite its obvious value. A key factor in the leaky inactivation phenotype observed for Uba1 mutants is the nature of the Uba1 protein itself, as an essential activator of all ubiquitin-dependent processes. Furthermore, it is known that the E1 reaction is much faster than downstream conjugation reactions (Pickart and Cohen 1994). Because the activation of E1 is not rate limiting, a leaky mutant may provide enough E1 activity to drive most ubiquitin-dependent processes without resulting in an observable change in proteolysis. Therefore, decreasing the abundance or activity of E1 enzyme could affect various E1-dependent cellular processes differently.

Certainly one reason for the lack of a distinctly severe proteolytic defect is that most existing *uba1* alleles had arisen spontaneously in the course of other, indirect "forward genetic" screens. For example, *uba-165* was isolated as a suppressor of *mcm3-10* when it was found to restore the interaction of Mcm3-10 mutant protein with other subunits of the MCM (minichromosome maintenance) complex, which is involved in DNA replication (Cheng et al. 2002). However, it would be surprising to isolate an E1 allele with a broad defect in proteolysis as a spontaneous mutation in such a specific screen. A defect in E1 ubiquitin activation would be expected to affect many ubiquitin-dependent processes, including DNA repair, translation, and endocytosis, in addition to proteolysis.

The leaky Uba1 inactivation in existing *uba1* mutant strains motivated our initial "reverse genetic" screen, in which we directly mutagenized the UBA1 gene. Although this screen identified fifty temperature-sensitive alleles, only four displayed a clear defect in

proteolysis. This result mirrors those from the original hydroxylamine mutagenesis of UBA1 (McGrath, 1991). Similarly, the *uba1-2* allele was isolated in a screen for defects in Deg1-βgal degradation, yet other proteins were only mildly stabilized (Swanson and Hochstrasser 2001). Based on these results, we hypothesize that most mutant alleles may target specific interactions between E1 and the many diverse E2 enzymes, thus inactivating only subsets of the overall ubiquitin-proteasome pathway. Indeed, *in vitro*, the rates of thiol ester formation from E1 to various purified E2 enzymes differs (Haas et al. 1988). This may explain the finding that in most E1 mutants, while turnover of specific proteins is inhibited, there is no severe defect in bulk ubiquitination, a result first seen in mammalian E1 mutants. The A31N-ts20 mutant showed a dramatic reduction in E1 to only 5%-10% of the original amount. This resulted in reduced ubiquitin conjugation onto specific proteins, such as p53 and c-Jun, but very mild reduction in bulk ubiquitin-protein conjugates (Salvat et al. 2000).

Based on our understanding of these previously isolated mutants, we incorporated two key features into the design of our genetic screen. First, a large library of *uba1* mutants with a broad mutation profile was created using the Stratagene Genemorph II Random Mutagenesis Kit. This system utilizes two different polymerase enzymes to introduce a uniform mutational profile, generating a similar frequency of A and T mutations and C and G mutations. In addition, the mutational frequency can be controlled by modulating the ratio of polymerase to target DNA. We created a library with a mutational range from 1 to 20 mutations per thousand base pairs. Directed evolution studies often use mutational frequencies of between 1 and 4 amino acid changes per protein (You and Arnold, 1996), while proteins with improved activity have been isolated with up to 20

mutations per protein (Daugherty et al. 2000). The *uba1-204* allele was the result of a mutation rate of 4.6 mutations/kb. In addition, error-prone PCR is preferential to less-efficient methods used to create earlier alleles, such as hydroxylamine mutagenesis, which only gives G:C and A:T transitions (McGrath, 1991), and upstream transposon insertion, which does not alter the coding sequence (Swanson and Hochstrasser 2001). Using this error-prone PCR strategy, we created a larger library of *uba1* mutants to screen for the most severe phenotype.

The second key step in isolating a strong loss-of-function mutant from this large library was our screening method. Based on the observation that in most E1 mutants specific substrates are stabilized while turnover of others is unaffected, we analyzed our resulting fifty candidate mutants by following the turnover of multiple diverse substrate proteins. Therefore, *uba1-204* is a unique allele of E1 in that it was the product of direct mutagenesis of the wild-type gene, and was isolated by screening for broad defects in proteolysis.

While the structure for the *S. cerevisiae* E1 protein has not been solved, the crystal structure of similar activating enzymes can provide clues into the structural features present in Uba1. *Escherichia coli* MoeB and MoaD proteins are involved in molybdenum cofactor biosynthesis, and their catalysis reactions are mechanistically similar that of E1. Active site residues 1 to 250 and 400 to 660 of MoeB are 17% and 22% similar to human UBA1, respectively (Lake et al. 2001), and MoaD displays the same fold and C-terminal Gly-Gly motif as ubiquitin (Rudolph et al. 2001). Indeed it is believed that these genes and ubiquitin and E1 may be derived from related ancestral genes (Rajagopalan 1997). When comparing the *Saccharomyces cerevisiae UBA1* sequence to the multiple sequence alignment of MoeB and human E1, only one mutation, V502A, lies in a region for which a

structural role has been assigned. This residue is conserved in the human sequence and resides adjacent to alpha helix 4, which is known to interact with the ATP molecule.

The structure of Uba3-APPB1, the activating enzyme for the ubiquitin-like protein NEDD8, has also been solved and can provide clues into possible structural features of Uba1 (Walden et al. 2003). When comparing these structures to the known sequence of *uba1-204*, it again become clear that the V520A mutation in helix 4 disrupts a residue that is known to contact the adenylation domain in the structurally similar Uba3-APPBP1 complex (Walden et al. 2003). In addition, the N630G mutation lies near the active-site cysteine in loop 9 and may affect protein folding necessary for the interaction with ubiquitin. While it is unclear how these specific mutations alter protein folding or activity, it is noteworthy that of the eight mutations found in the *uba1-204* sequence, four of them result in replacement of an acidic residue with glycine. Current research being done on the structure of E1, as well as other structurally similar proteins such as Uba3-APPB1 and the MoeB complex, may help to shed light on the functional consequences of mutating specific residues of these activating enzymes.

MATERIALS AND METHODS

Generation of mutant alleles

Error-prone PCR was done using Genemorph II Random Mutagenesis Kit (Stratagene, La Jolla, CA) according to protocols listed in the product specifications, using a target DNA amount ranging from <0.1ng to 1000ng in order to produce a wide range of mutation frequencies. A large amount of target DNA (500-1000ng) is recommended to

achieve a low mutation frequency (0-4.5 mutations/kb), while using a lower amount of target DNA (0.1-100ng) results in higher mutation rates (>9 mutations/kb). The target DNA used was RDB1837, which contained wild-type UBA1 cloned from W303 *S. cerevisiae* cell and primers used for amplification were NG19 (5'-CCGCTCGAGGGTAAAGTGGTTGAGCGAGGTA-3') and NG20 (5'-GGACTAGTGAATTGCCATTACGCTTCC-3'; *Xho*I and *Spe*I sites underlined). The mutant *uba1* gene products from the various PCR reactions were pooled and cotransformed into RJD3268 cells, along with pRS313 plasmid that had been linearized with *Nhe*I.

A plasmid shuffling strategy was used to isolate cells that contained a genomic deletion of the essential UBA1 gene and carried only a mutant copy of the gene. The entire coding region at one locus in a diploid W303 wild-type yeast strain was replaced with the KanMX marker, cells were grown in YPD for 12 hours to permit expression of KanMX, and selected by plating onto YPD plates containing 200 μg/ml Geneticin G-418 Sulfate (Invitrogen, Carlsbad, CA). Gene disruption was verified by PCR and by sporulation and tetrad dissection. The resulting strain also contained a partial deletion of the overlapping Ste6 gene, causing sterility in mating type a cells.

Transformants were plated onto –His plates to select for gapped plasmids which had recombined with *uba1* PCR product and later replica plated onto plates containing 5-fluoro-orotic acid in order to isolate clones which had lost the *URA3* plasmid.

Isolation of plasmids from yeast cells for sequence analysis

Yeast strains were grown to log phase at 25°C in rich medium and a 1.5 ml aliquot was centrifuged. Plasmids were rescued using the QIAprep Spin Miniprep Kit (Qiagen,

Valencia, CA). Cell pellets were resuspended in 250 ul buffer P1 and 250 ul glass beads and vortexed for 5 minutes. 350 ul of buffer N3 was immediately added and samples were centrifuged for 10 minutes at high speed. Supernatant was applied to QIAprep spin column and centrifuged for 45 seconds. Column was washed with 750 ul of buffer PE and centrifuged for 45 seconds. Column was placed in a clean tube and 50 ul of buffer EB was used to elute plasmid DNA by centrifuging sample for 1 minute. 1-2 ul of the resulting sample was used to transform *E. coli* cells. Plasmids were purified from these transformed bacterial cells and sequenced.

Ubiquitination and degradation assays

Described in detail in chapter 3, materials and methods.

Chapter 3

A CONDITIONAL YEAST E1 MUTANT BLOCKS THE UBIQUITIN-PROTEASOME PATHWAY AND REVEALS A ROLE FOR UBIQUITIN CONJUGATES IN TARGETING RAD23 TO THE PROTEASOME

(Published in Molecular Biology of the Cell, **18**, 1953-1963)

ABSTRACT

E1 ubiquitin-activating enzyme catalyzes the initial step in all ubiquitin-dependent processes. We report the isolation of *uba1-204*, a temperature-sensitive allele of the essential *S. cerevisiae* E1 gene, *UBA1*. *Uba1-204* cells exhibit dramatic inhibition of the ubiquitin-proteasome system, resulting in rapid depletion of cellular ubiquitin conjugates and stabilization of multiple substrates. We have employed the tight phenotype of this mutant to investigate the role ubiquitin conjugates play in the dynamic interaction of the UbL/UBA domain adaptor proteins Rad23 and Dsk2 with the proteasome. Although proteasomes purified from mutant cells are intact and proteolytically active, they are depleted of ubiquitin conjugates, Rad23, and Dsk2. Binding of Rad23 to these proteasomes *in vitro* is enhanced by addition of either free or substrate-linked ubiquitin chains. Moreover, association of Rad23 with proteasomes in mutant and wild-type cells is improved upon stabilizing ubiquitin conjugates with proteasome inhibitor. We propose that

recognition of polyubiquitin chains by Rad23 promotes its shuttling to the proteasome *in vivo*.

INTRODUCTION

Activation of ubiquitin by ubiquitin-activating enzyme (E1) is the requisite first step in all ubiquitin-dependent pathways, including regulated proteolysis. The process begins with an ATP-dependent reaction in which the ubiquitin moiety forms a high-energy thioester bond with the active-site cysteine of E1. E1 can then transfer the activated ubiquitin to a conjugating enzyme (E2), which acts alone or in conjunction with a ubiquitin ligase (E3) to covalently link ubiquitin to lysine residues on specific target proteins (Haas and Siepmann, 1997). Through successive ligation reactions, a polyubiquitin chain can form on the substrate and serve as a signal for targeting to the multisubunit 26S proteasome. Composed of a cylindrical 20S proteolytic core complex capped at one or both ends by 19S regulatory complexes, the proteasome deubiquitinates and unfolds substrates before translocating them into its core for proteolysis (Amerik and Hochstrasser 2004; Pickart and Cohen 2004).

The existence of mammalian cell lines that carry temperature-sensitive alleles of E1 has been of great importance to the study of the functions of the ubiquitin system in animal cells (Finley et al. 1984; Ciechanover et al. 1984; Kulka et al. 1988; Salvat et al. 2000). Ironically, no tight, rapid-acting conditional mutation has been described for the budding yeast *UBA1* gene that encodes E1 despite the availability of sophisticated molecular genetic techniques in this organism. Although a temperature-sensitive allele of *UBA1* exists, this allele results in only moderate stabilization of tested substrates, and

possible defects in ubiquitination were not examined (McGrath 1991; Gandre and Kahana 2002). A second allele resulting from a transposon insertion upstream of the *UBA1* coding sequence reduced wild-type Uba1 protein function, causing inefficient degradation of some proteins (Swanson and Hochstrasser 2000). Additional alleles were later encountered as suppressor mutations in various indirect genetic screens and also achieved only partial inactivation of the pathway (Cheng et al. 2002; Shimada et al. 2002). Whereas these hypomorphic alleles have proven useful in confirming the ubiquitin dependence of the turnover of specific proteins, they highlight the potential value of a stronger conditional allele with broad utility in exploring the entire ubiquitin conjugation pathway. Among the many issues that could be addressed with a tight and rapid-acting temperature-sensitive mutation in *UBA1* is the question of how ubiquitin conjugates contribute to the proteasomal targeting of substrates destined for proteolysis.

While the enzymatic cascade responsible for polyubiquitination provides strict control of substrate tagging, the pathway was originally thought to culminate in a stochastic interaction between polyubiquitin chains and the proteasome. On the contrary, recent work has shown that a diverse set of ubiquitin-binding receptors regulate the targeting of ubiquitinated proteins to the proteasome in a substrate-specific manner (Chen and Madura 2002; Elsasser et al. 2004; Verma et al. 2004; Wilkinson et al. 2001; reviewed in Elsasser and Finley 2005; Hicke et al. 2005). The first polyubiquitin-binding receptor identified was Rpn10, a subunit of the 19S regulatory complex that contains a ubiquitin-interacting motif (UIM) (Deveraux et al. 1994). However, cells lacking Rpn10 exhibit only mild phenotypes, indicating that additional ubiquitin chain recognition mechanisms must exist (van Nocker et al. 1996). A second class of polyubiquitin binding proteins, referred to as UbL/UBA proteins, is exemplified in yeast by the nucleotide excision repair protein

Rad23 (Watkins et al. 1993) and the spindle pole duplication factor Dsk2 (Biggins et al. 1996). UbL/UBA proteins specifically recognize polyubiquitin chains via C-terminal ubiquitin-associated (UBA) domains (Bertolaet et al. 2001b; Wilkinson et al. 2001; Hofmann and Bucher, 1996; Rao and Sastry 2002; Chen and Madura 2002; Raasi and Pickart 2003). For example, Rad23 has two UBA domains that interact with polyubiquitinated proteins in a linkage-specific and chain length-dependent manner, preferentially binding to the K48-linked ubiquitin chains that serve as a degradation signal (Raasi and Pickart 2003). In addition, these proteins interact with the proteasome via their N-terminal ubiquitin-like (UbL) domain (Walters et al. 2002; Schauber et al. 1998; Elsasser et al. 2002; Saeki et al. 2002).

Integrating these two recognition motifs, UbL/UBA proteins, like Rpn10, are proposed to function as receptors that link polyubiquitinated proteins to the proteasome. Several lines of evidence support this receptor hypothesis. In *rad23* and *dsk2* mutant cells, substrates are ubiquitinated but not degraded, consistent with a role in substrate delivery (Chen and Madura 2002; Funakoshi et al. 2002; Lambertson et al. 1999; Rao and Sastry 2002; Saeki et al. 2002; Wilkinson et al. 2001). Moreover, both the UbL and UBA domains of Rad23 are essential for its role in promoting proteolysis (Lambertson et al. 2003; Bertolaet et al. 2001b; Rao and Sastry 2002). Most recently, it was shown that Rad23 and Rpn10 can directly promote proteasome binding and degradation of a ubiquitinated substrate *in vitro*, thereby establishing a direct receptor function for these proteins (Verma et al. 2004).

UbL/UBA proteins are emerging as central players in selective proteolysis, and their interactions with numerous other ubiquitin-proteasome system (UPS) elements suggest a complex regulatory scheme, which remains poorly understood. For example,

there are reports that UbL/UBA proteins may regulate substrate ubiquitination as well as proteasomal targeting. The UbL domain of Rad23 binds the ubiquitin ligase Ufd2, which cooperates with the chaperone-like AAA ATPase Cdc48 and its cofactors to ubiquitinate specific substrates (Richly et al. 2005; Kim et al. 2004; Schuberth et al. 2004). Moreover, when overexpressed, Rad23 and Dsk2 are capable of inhibiting proteolysis by binding a polyubiquitin chain on a substrate and inhibiting the ligation of additional ubiquitin molecules (Kleijnen et al. 2000; Ortolan et al. 2000). Even the stoichiometry of receptor-ubiquitin chain interactions is potentially complex given that Rad23 can form homodimers as well as heterodimers with the UbL/UBA protein Ddi1 (Bertolaet et al. 2001a; Bertolaet et al. 2001b; Kang et al. 2006) and that one polyubiquitin chain may simultaneously capture two receptor molecules (Kang et al. 2006; Lowe et al. 2006). Finally, intramolecular interactions between UbL and UBA domains may function in regulating UbL/UBA protein activity (Walters et al. 2003; Ryu et al. 2003; Raasi et al. 2004).

In this study, we isolate and characterize a novel allele of the yeast *UBA1* gene, *uba1-204*, in which ubiquitin molecules are not efficiently assembled into chains or conjugated onto substrates. We employ the resulting ubiquitin chain-depleted cellular environment to investigate the nature of ubiquitin-dependent proteasomal targeting.

RESULTS

Isolation and phenotypic analysis of uba1-204

The initial goal of this study was to create a loss-of-function allele of the *S. cerevisiae* ubiquitin-activating enzyme that resulted in strong and rapid inactivation of ubiquitin conjugation. To generate mutant alleles, the *UBA1* coding sequence, carried on a *HIS3* plasmid and expressed from the natural *UBA1* promoter, was subjected to random PCR mutagenesis. Mutant plasmids were introduced into *uba1Δ* haploid cells sustained by a low copy *URA3* plasmid containing *UBA1*. Transformants were plated on 5-fluoro-orotic acid to evict the *UBA1* plasmid and clones sustained by the mutagenized plasmid were sought. In a screen for temperature-sensitive growth, fifty candidate mutant alleles that grew at 25°C but failed to grow at 37°C were isolated. To identify mutants that exhibited broad defects in the ubiquitin-proteasome system, we tested these alleles for loss of ubiquitin conjugates at the nonpermissive temperature. Whereas the majority of these *uba1* mutants largely retained ubiquitin conjugates at the nonpermissive temperature, *uba1-204* mutant cells rapidly lost ubiquitin conjugates upon transfer to 37°C (data not shown). The *uba1-204* mutant gene was sequenced and found to contain mutations leading to eight amino acid alterations: D318G, K401E, V502A, E523G, E534G, N630G, F680S, D936E. Although none of the mutations occurred in close proximity to the adenylation site or the active-site cysteine, four mutations resulted in the replacement of acidic residues with glycine.

Cellular viability was unaffected in *uba1-204* cells grown at temperatures ranging from the 25°C permissive temperature up to 33°C (Figure 3-1A). Mutant cells began to exhibit loss of viability at 35°C and were completely inviable at 37°C (Figure 3-1A). Sensitivity to environmental stress is often a hallmark of ubiquitin pathway mutations, because stress leads to an increased requirement for protein quality control. As predicted, compromised Uba1 activity conferred sensitivity to the cellular stressor cadmium chloride (Figure 3-1B). Another important feature of the UPS is its critical role in the regulation of cell-cycle progression. Whereas mammalian E1 mutants arrest at S/G2 (Finley et al. 1984; Kulka et al. 1988; Goebl et al. 1988), the cold-sensitive yeast *uba1-165* mutant has a G1 arrest phenotype (Cheng et al. 2002) and existing temperature-sensitive yeast E1 mutants do not display a cell-cycle phenotype (McGrath, 1991; Swanson and Hochstrasser 2000). In *uba1-204* mutants, cellular division ceased within one cell-cycle of shifting cells to the nonpermissive temperature (data not shown). To test the influence of the *uba1-204* mutation on the cell-cycle, cellular DNA content was assessed by flow cytometric analysis. When unsynchronized *uba1-204* cultures were incubated at the nonpermissive temperature, a G2 arrest phenotype was apparent, with some cells continuing through the cell-cycle to arrest in G1 (Figure 2-10). Next, we synchronized cells in G1 with α-factor prior to shifting them to 37°C. Upon release into fresh medium at the nonpermissive temperature, wild-type cells progressed through the cell-cycle while uba1-204 cells remained arrested at G1 (Figure 3-1C). By contrast, when α-factor synchronized cells were released into fresh medium at the permissive temperature for 90 minutes to allow progression through the cell-cycle prior to shifting to 37°C, uba1-204 cells arrested at

G2 while wild-type cells did not (Figure 3-1D). Therefore, *uba1-204* mutant cells arrest at both G1 and G2 of the cell-cycle.

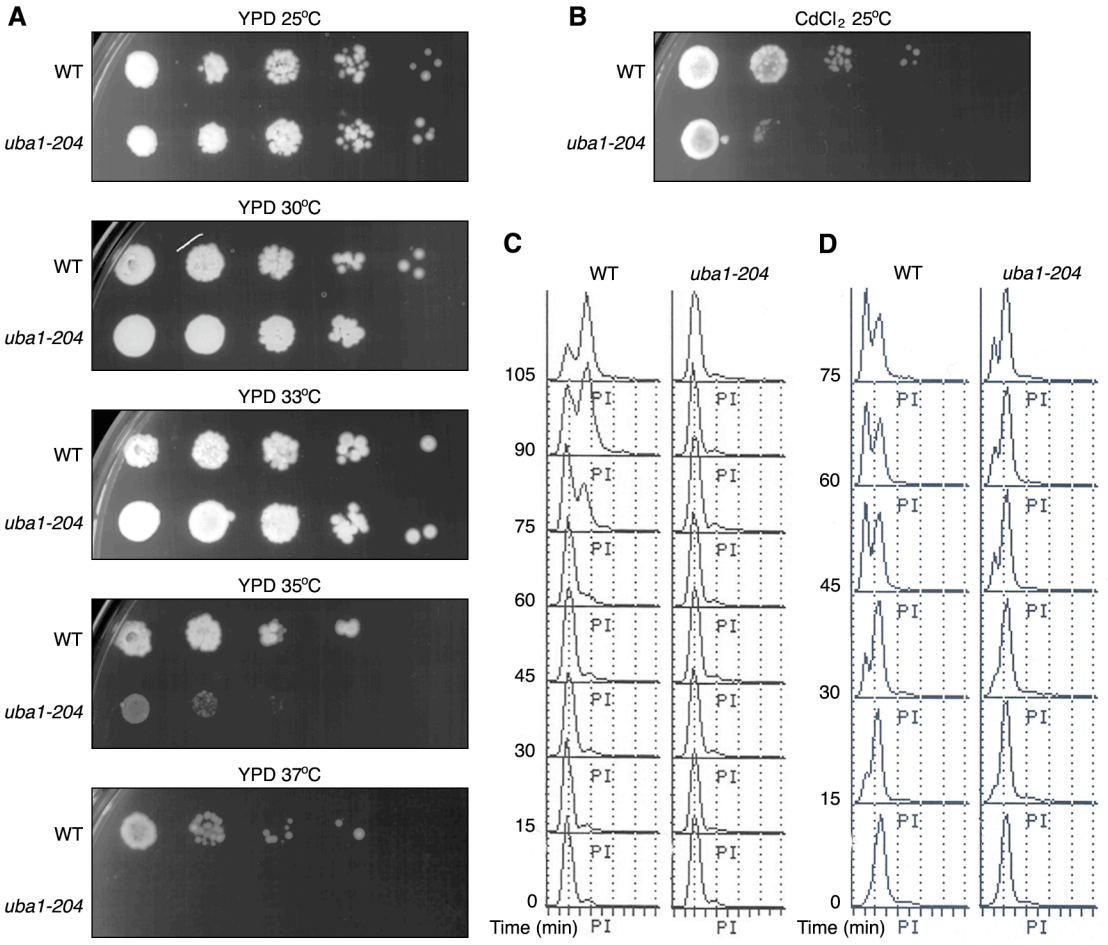

Figure 3-1: *Uba1-204* cells are temperature-sensitive and undergo cell-cycle arrest. (A) Ten-fold serial dilutions of wild-type and *uba1-204* yeast cells were spotted onto YPD and (B) SD plates containing 30 μM $CdCl_2$ and incubated at the indicated temperatures for 2-3 days. (C) Wild-type and *uba1-204* cells were arrested with α-factor for 2 hours at the permissive temperature. The

temperature was shifted to 37°C for 1 hour and the cells were released into fresh medium at 37°C at time 0. At indicated time points following release, aliquots were withdrawn and prepared for assessment of total DNA content by fluorescence-activated cell sorting (FACS). (D) WT and *uba1-204* cells were arrested with α-factor for 3 hours at the permissive temperature. Cells were then released into fresh medium and grown at 25°C for 90 minutes to allow progression to G2 phase. Cells were then shifted to 37°C at time 0 and aliquots were withdrawn and analyzed as in C.

Uba1-204 cells are defective in ubiquitin conjugation and substrate degradation

Complete inactivation of Uba1 should yield universal shutdown of downstream ubiquitination pathways. To determine the extent of impairment to the UPS, the effect of the ubiquitin activation defect on overall ubiquitin conjugate accumulation was monitored. Strikingly, a nearly complete loss of detectable ubiquitin conjugates was observed within five minutes of shifting the cells to 37°C (Figure 3-2A). The temperature-dependent defect in ubiquitin conjugate accumulation was partially reversed when cell cultures that were incubated at 37°C for one hour were returned to 25°C (Figure 3-2B). To determine the impact of this reversibility on future experiments, we evaluated the restoration of ubiquitination activity in mutant cells incubated on ice. Unexpectedly, it was observed that in *uba1-204* cultures which were incubated at 37°C and then placed on ice, ubiquitin conjugates began to reappear within minutes (Figure 3-2C). Therefore, to ensure full Uba1 inactivation in all future experiments, wild-type and mutant cells were maintained at

the restrictive temperature throughout centrifugation and preparation steps until they were flash-frozen in liquid nitrogen.

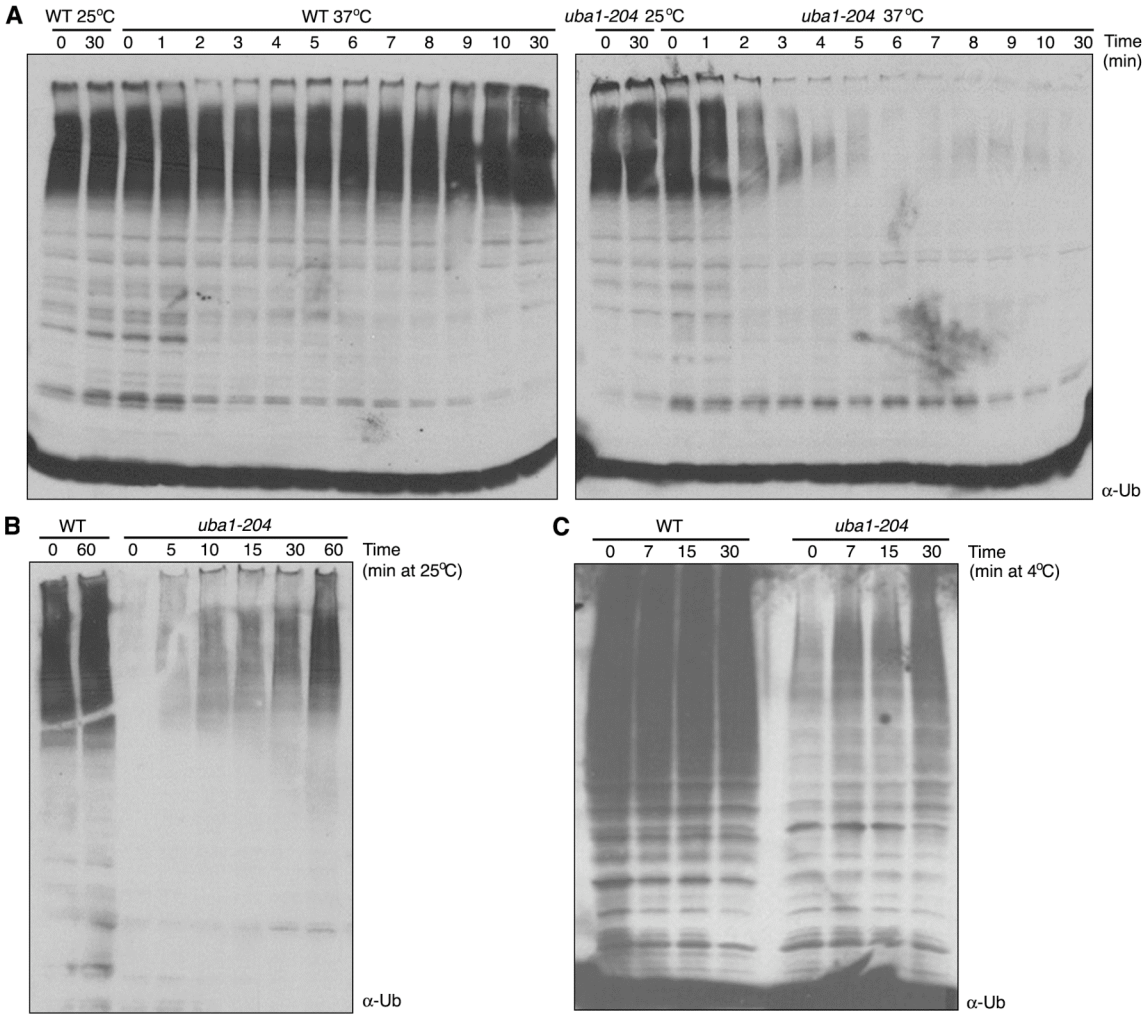

Figure 3-2: *Uba1-204* cells are defective in ubiquitin conjugation. (A) Wild-type and *uba1-204* cells were grown to log phase in liquid YPD medium at 25°C. Half of each culture was shifted to the nonpermissive temperature at time 0 and samples were withdrawn every minute. Lysates were prepared and analyzed by

SDS-PAGE and immunoblotted with antiserum to ubiquitin. (B) Loss of ubiquitin conjugation is reversible. Strains were grown as in A and samples were shifted to the nonpermissive temperature for 1 hour. At time 0, the temperature was shifted back to 25°C, aliquots were withdrawn at indicated time points and ubiquitin conjugation was assessed as in A. (C) *Uba1-204* cells are active in ubiquitin conjugation at 4°C. Cells were grown in YPD medium and shifted to 37°C for 1 hour. At time 0, ice was added to cultures and the temperature was shifted to 4°C. Samples were withdrawn and analyzed as in A

The dramatic reduction in ubiquitin conjugate levels in *uba1-204* cells at the nonpermissive temperature indicates that multiple downstream E2/E3 pathways were inactivated. If this was indeed the case, stabilization of diverse proteasome substrates would be expected. To test this, the turnover of a synthetic substrate, Deg1-GFP, was analyzed in a cycloheximide chase experiment. Deg1-GFP bears the degradation signal from the rapidly degraded Matα2 protein and is a substrate for the ubiquitin ligase Doa10 (Swanson et al. 2001). At 25°C, the majority of Deg1-GFP was destroyed within 15 minutes of terminating protein synthesis in both wild-type and mutant strains (Figure 3-3A). The protein was modestly stabilized in the wild-type cells at 37°C, but was completely stabilized in the *uba1-204* cells at 37°C. To examine the scope of this proteolytic defect, we also monitored turnover of Ub^{V76}-V-βgal, a cytosolic substrate of the UFD ubiquitin ligase pathway (Johnson et al. 1995). Although degradation of Ub^{V76}-V-βgal occurred with normal kinetics following a galactose promoter shut-off in the mutant cells at 25°C, there

was no detectable degradation of the substrate in *uba1-204* cells at 37°C (Figure 3-3B). In addition, ubiquitin-protein conjugates could be detected in the early time points of the wild-type samples at both temperatures and in the mutant samples at 25°C. However, these conjugates were conspicuously absent in *uba1-204* cells at 37°C.

To determine the physiological significance of these turnover defects, we also assessed the effect of impaired ubiquitin activation on a well-characterized endogenous substrate, the cyclin-dependent kinase inhibitor Sic1. At the G1/S boundary, Sic1 is polyubiquitinated by the SCF ubiquitin ligase and then degraded by the proteasome (reviewed in Deshaies, 1999). Wild-type and mutant cells carrying a *GAL-SIC1* allele were arrested with α-factor, Sic1 expression was transiently induced with a pulse of galactose, and cells were released from G1 into the cell-cycle. Similarly to the test substrates, Sic1 degradation was not impaired in *uba1-204* cells at the permissive temperature, but the protein was stabilized at 37°C (Figure 3-3C). These data confirm that in the *uba1-204* mutant, multiple downstream proteolytic pathways were inhibited.

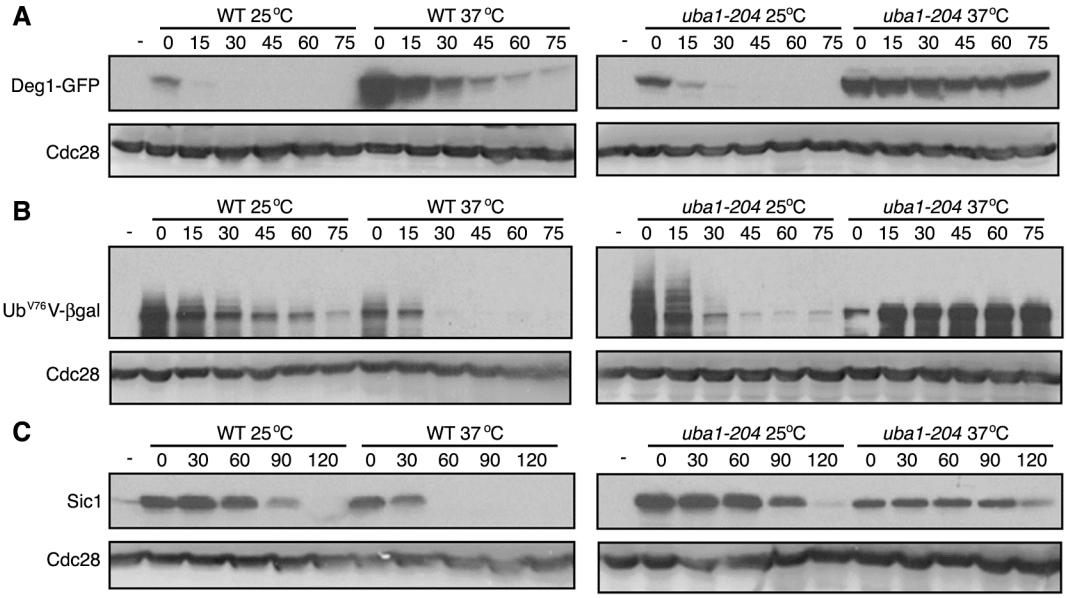

Figure 3-3: *Uba1-204* cells are defective in substrate degradation. (A) Wild-type and *uba1-204* cells expressing Deg1-GFP were grown in SD medium. Cultures of exponentially growing cells were incubated at 25°C or shifted to 37°C for 1 hour and cycloheximide was added to initiate a chase period. Samples were withdrawn every fifteen minutes for analysis. Lysates were separated by SDS-PAGE and immunoblotted with antiserum to GFP. Control (-) sample was an isogenic strain lacking the plasmid. (B) WT and *uba1-204* cells expressing Ub^{V76}-V-βgal under control of the *GAL1* promoter were grown in SD medium with raffinose and protein expression was induced by addition of 2% galactose for 1 hour. Cultures were then incubated at either 25°C or shifted to 37°C for 1 hour and transferred to dextrose medium pre-equilibrated at the same temperature to initiate a chase. Samples were withdrawn every 15 minutes, lysed, separated by SDS-PAGE and immunoblotted with antiserum to β-gal. (C) WT and *uba1-*

204 cells expressing Sic1 under the control of the *GAL1* promoter were grown in SD medium with raffinose and arrested with α-factor for 2 hours. Sic1 expression was induced by addition of galactose to 2% and cells were incubated at 25°C for 1 hour before shifting to 37°C for an additional hour. Cells were then transferred to dextrose medium to initiate a chase and samples were withdrawn every 30 minutes, lysed, separated by SDS-PAGE and immunoblotted with antiserum to Sic1. Protein loading was verified by immunoblotting with antiserum to Cdc28.

Uba1-204 cells contain intact and active proteasomes

To address the impact of a ubiquitin activation defect further downstream in the ubiquitination pathway, we examined its affect on the proteasome. Considering that many subunits of the proteasome can be ubiquitinated (Peng et al. 2003) and the proteasome has been suggested to undergo rapid cycles of assembly/disassembly (Babbitt et al. 2005), we first investigated a possible role for polyubiquitination in the maintenance of fully assembled 26S proteasome complexes. When the chromosomal locus encoding Pre1, an alpha subunit of the 20S core, is replaced by an allele tagged with a Flag epitope, it is possible to obtain intact, active 26S proteasome complexes by a single-step affinity purification method (Verma et al. 2000). Proteasomes affinity purified from *uba1-204* cells cultured at either 25 or 37°C were found to contain all 20S and 19S subunits with no detectible change in subunit composition (Figure 3-4A). Quantitative mass spectrometric analysis of these samples also showed no significant alteration in subunit abundance in proteasomes purified from the mutant strain (data not shown). The assembly state of the

purified proteasomes was further confirmed by subjecting samples to native gel electrophoresis. Coomassie blue staining showed intact 20S core particle (CP) complexes as well as proteasomes with either one (R_1P) or two (R_2P) 19S regulatory particles attached (Figure 3-4B). The ratios of various proteasomal subcomplexes in the mutant were comparable to that seen in wild-type. Thus, a robust level of ongoing ubiquitination is not necessary to sustain proteasome complexes *in vivo*, making it possible to purify intact proteasomes from *uba1-204* mutant cells.

Next, we examined the functional consequences of E1 inactivation on these intact proteasomes. Proteasome peptidase activity was tested by in-gel hydrolysis of the fluorogenic peptide substrate Suc-LLVY. Peptidase activity was similar for 20S and 26S proteasomes purified from wild-type and *uba1-204* cells (Figure 3-4C). Purified 26S proteasomes were next evaluated for their ability to degrade a polyubiquitinated physiological substrate, Sic1 (Ub-Sic1). High molecular-weight Ub-Sic1 conjugates were completely degraded upon incubation with proteasomes isolated from wild-type or *uba1-204* cells (Figure 3-4D). Inhibition of proteolysis with the 20S proteasome inhibitor epoxomicin resulted in accumulation of deubiquitinated Sic1 (Figure 3-4D) (Verma et al. 2002).

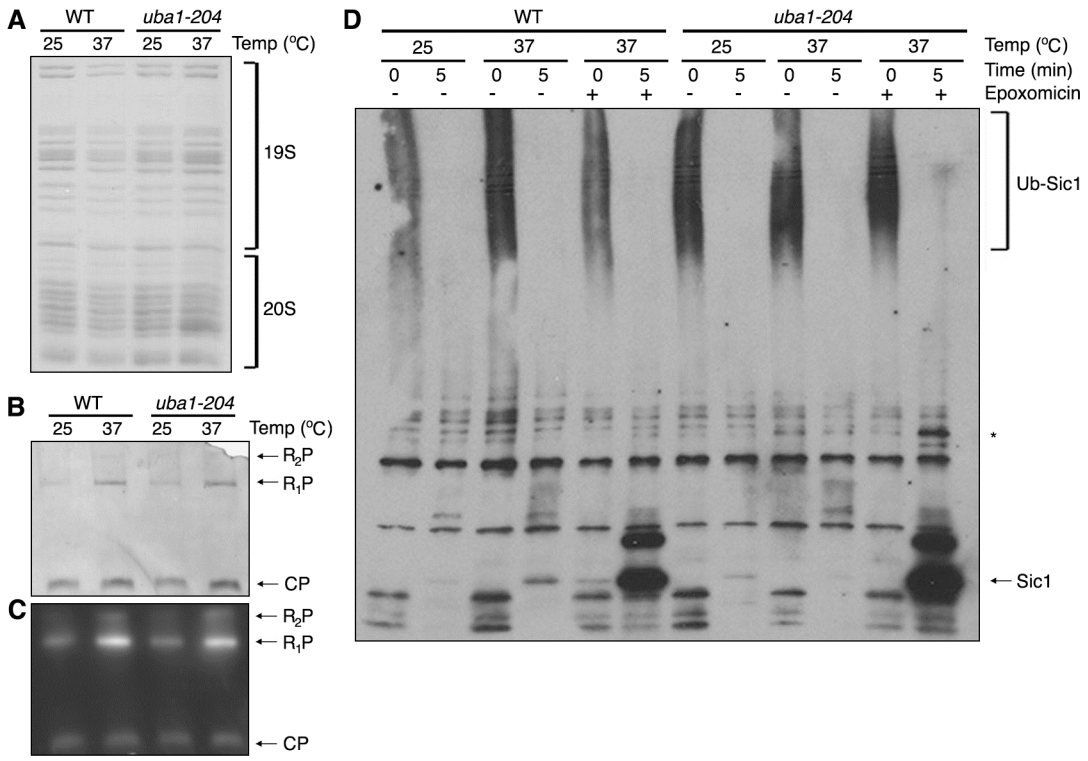

Figure 3-4: 26S proteasomes isolated from *uba1-204* cells are properly assembled and proteolytically active. (A) Intact 26S proteasomes can be purified from *uba1-204* cells. Wild-type and *uba1-204* cells were incubated at 25°C or 37°C for 40 minutes and 26S proteasomes were affinity purified as described in materials and methods. Samples were resolved by SDS-PAGE and visualized by Coomassie blue staining. 19S and 20S subunits are specified. (B) Purified proteasome complexes were resolved by nondenaturing PAGE and were visualized by Coomassie blue staining. CP refers to 20S core particle, and R_1P and R_2P refer to 26S proteasomes with one or two regulatory caps, respectively. (C) Proteolytic activity of the complexes in the nondenaturing gel from B was detected by fluorogenic peptide overlay with the peptidase substrate

Suc-LLVY-AMC. Fluorescent bands were visualized by exposure to UV light. (D) *Uba1-204* 26S proteasomes are active in the degradation and deubiquitination of Ub-Sic1 *in vitro*. 26S proteasomes purified from wild-type and *uba1-204* cells were incubated with Ub-Sic1 at 30°C for 5 minutes. For deubiquitination reactions, proteasomes were preincubated with 100 μM epoxomicin for 30 minutes at 30°C prior to incubation with Ub-Sic1. Samples were analyzed by SDS-PAGE followed by immunoblotting with anti-Sic1 antibody. Polyubiquitinated Sic1 (Ub-Sic1) and deubiquitinated Sic1 are specified. There is a band of unknown identity (*) that was reproducibly detected in the mutant but not wild-type lanes in the presence of epoxomicin.

Ubiquitin-binding proteins have differential requirements for polyubiquitin in proteasome targeting

Having established that cellular depletion of polyubiquitin chains does not alter proteasome activity, we next evaluated the association of known ubiquitin-binding factors with the proteasome. Cell lysates were prepared from wild-type and mutant cells, and proteasome complexes were purified by immunoprecipitation as described. Comparable levels of the 20S proteasome subunit Pre2 (tested with antibody to LMP7, the human homolog) were detected in all immunoprecipitation samples, verifying that equivalent amounts of intact proteasomes were purified from wild-type and *uba1-204* cells (Figure 3-5E). As expected, there was a striking decrease in the association of ubiquitin conjugates with the 26S complex isolated from *uba1-204* cells held at 37°C (Figure 3-5A). Although

Rpn10 is the only validated ubiquitin-binding proteasome subunit, most cellular Rpn10 remains free, unincorporated into proteasome complexes (van Nocker and Vierstra, 1993; Deveraux et al. 1994; Haracska and Udvardy 1995). This had suggested the possibility that Rpn10, as well as Rad23 and Dsk2, may form transient interactions with the proteasome, cycling between a free and assembled form. We therefore examined how the defect in ubiquitination impacted this potential equilibrium. Analysis of purified proteasomes indicated that loss of polyubiquitination activity in *uba1-204* cells did not alter Rpn10 incorporation into the proteasome complex (Figure 3-5D). These data, verified by mass spectrometry, suggest that the interaction of Rpn10 with polyubiquitin chains is not necessary for its association with intact proteasome complexes. In contrast, proteasomes isolated from *uba1-204* at the restrictive temperature exhibited a significant decrease in the amount of associated UbL/UBA proteins Rad23 (Figure 3-5B) and Dsk2 (Figure 3-5C). Meanwhile, overall levels of both Rad23 and Dsk2 proteins in mutant cell lysates were not affected by the temperature shift. Therefore, whereas both UbL/UBA receptor proteins were indeed present in cell lysates, they failed to associate efficiently with the proteasome upon inhibition of ubiquitin conjugate formation.

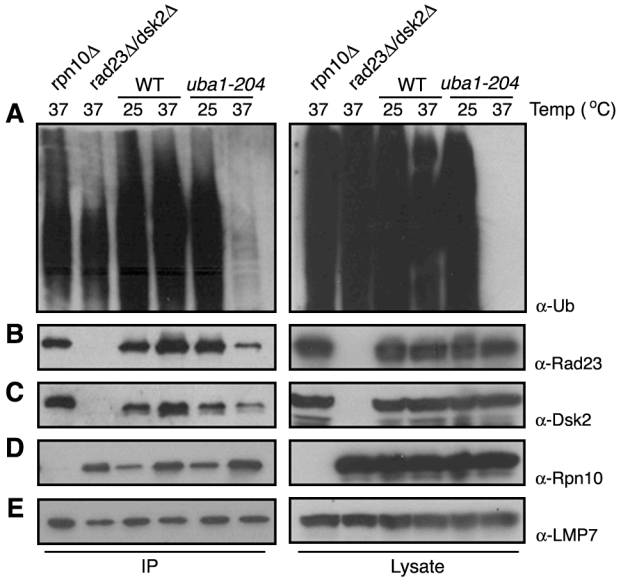

Figure 3-5: 26S proteasomes isolated from *uba1-204* cells exhibit reduced content of UbL/UBA proteins. (A-E) Wild-type and *uba1-204* cells expressing Pre1-FH were grown in casamino acid medium and half the cultures were shifted to 37°C for 40 minutes. Lysates were prepared and immunoprecipitated as described in materials and methods by incubation with anti-Flag resin in the presence of ATP. Intact 26S proteasomes were eluted with Flag peptide, separated by SDS-PAGE, and proteasome-bound proteins were detected by immunoblotting with antiserum to the specified proteins. Antibody specificity was verified using deletion mutants.

Ubiquitin chains promote Rad23 association with the proteasome

To examine the nature of ubiquitin conjugation-dependent receptor targeting in more depth, we focused on Rad23. The dual recognition capability of UbL/UBA proteins like Rad23 underlies their adaptor function, but it is unclear whether ubiquitin chain binding occurs before or after proteasome binding. The essentially ubiquitin-free nature of proteasomes purified from *uba1-204* cells presented an ideal reagent with which to examine the ubiquitin-dependence of Rad23 targeting. If the observed decrease in Rad23 interaction with the proteasome was truly a result of its inability to locate ubiquitinated substrates, addition of such substrates would be expected to restore binding. To test this hypothesis, we analyzed the effect of addition of the polyubiquitinated substrate, Ub-Sic1, on the ability of GST-Rad23 to bind to immobilized proteasomes *in vitro*. As the results in Figure 3-6A illustrate, addition of Ub-Sic1 resulted in a marked increase in the binding of full-length GST-Rad23 to proteasomes. A GST-UBA fusion protein that lacks the proteasome-binding UbL domain was unable to associate with the proteasome. Conversely, Rad23 lacking the UBA domains (GST-UbL) binds the proteasome regardless of whether Ub-Sic1 substrate is present (Figure 3-6A). The Ub-Sic1-dependence of GST-Rad23 targeting provides further support for the notion that Rad23 interaction with polyubiquitinated proteins can promote its shuttling to the proteasome. Furthermore, to ensure that this response was independent of the GST tag, Rad23 fused to a His_6 epitope was also tested with similar results (Figure 3-6B).

A recent report demonstrated that Ub-Sic1 is preferentially delivered to the proteasome by either Rad23 or Rpn10 (Verma et al. 2004). The capacity of Rad23 and other receptors to selectively target substrates for proteolysis suggests that in addition to

recognizing conjugated polyubiquitin chains, Rad23 may detect degradation signals within substrate proteins themselves. To determine if recognition of a polyubiquitin chain is sufficient to enhance binding of Rad23 to the proteasome, free K48-linked tetra-ubiquitin chains (Ub_4) were tested in the proteasome-binding assay. The results in Figure 3-6C demonstrate that Ub_4 was sufficient to stimulate GST-Rad23 recruitment to the proteasome and that the presence of conjugated substrate is not absolutely required to drive targeting *in vitro*. To extend these conclusions to a cellular environment, the proteasome inhibitor MG132 was used to stabilize polyubiquitin chains *in vivo*. Analysis of proteasomes from cells treated with the drug confirmed an increase in proteasome-bound Rad23 in both mutant and wild-type cells coincident with an increase in ubiquitin chains (Figure 3-6D).

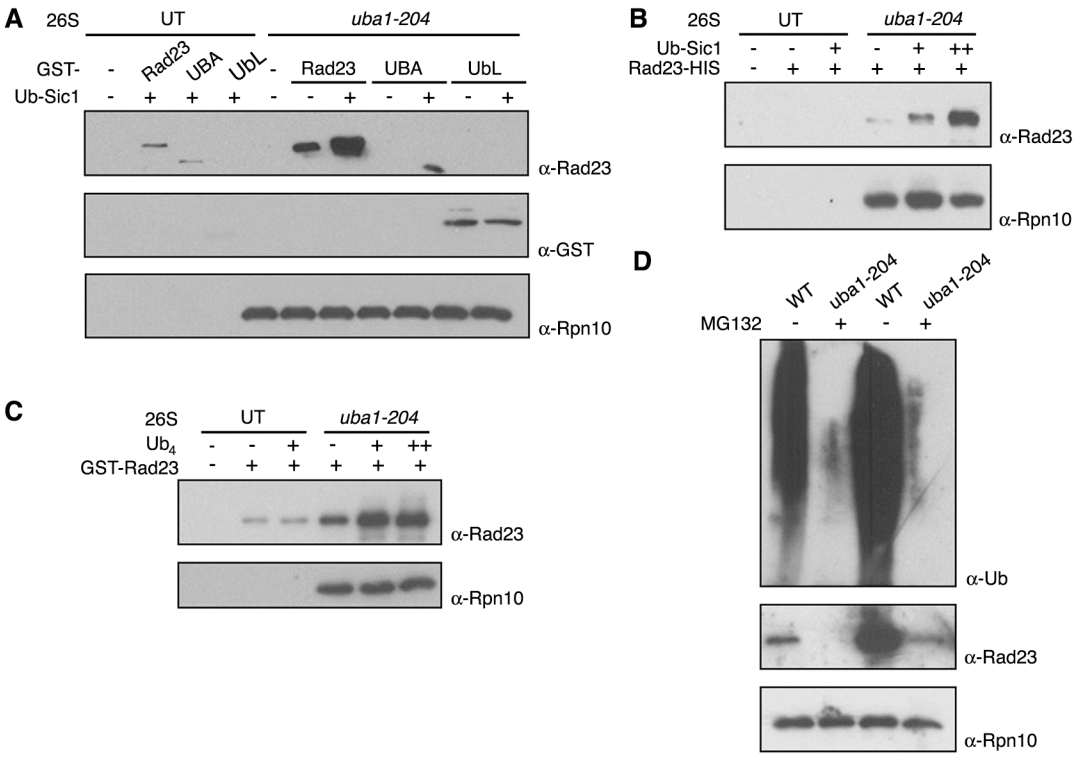

Figure 3-6: Polyubiquitin chains promote Rad23 binding to the proteasome. (A) Ub-Sic1 promotes association of full-length GST-Rad23 with proteasome. Sepharose-immobilized proteasomes isolated from *uba1-204* cells were preincubated with proteasome inhibitors for 1 hour and then incubated with GST fusion proteins in the presence or absence of Ub-Sic1 as described in materials and methods. GST-Rad23 refers to the full-length protein, whereas GST-UBA contains both UBA domains and lacks the UbL domain. GST-UbL contains only the N-terminal UbL domain and was detected with antiserum to GST. The presence of proteasome complexes was verified with antibodies to Rpn10. As a negative control, simultaneous purification was conducted with *uba1-204* cells lacking the Pre1-Flag allele (UT). (B) Ub-Sic1 promotes association of Rad23-

HIS with proteasome. Immobilized proteasomes were prepared as in A and incubated with Rad23-HIS in the presence or absence of Ub-Sic1. (C) Free tetraubiquitin chains are sufficient to promote GST-Rad23 association. Immobilized proteasomes were prepared as in A and incubated with GST-Rad23 and Ub_4 rather than Ub-Sic1. (D) Stabilization of polyubiquitin conjugates *in vivo* promotes Rad23 targeting to the proteasome. Wild-type and *uba1-204* cells were treated with MG132 or DMSO (-) and shifted to 37°C for 1 hour. Proteasomes were isolated by affinity purification, ubiquitin conjugates were detected with antiserum to ubiquitin, and Rad23 binding was assessed.

DISCUSSION

The initial goal of this study was to develop a method of inhibiting the entire ubiquitin-proteasome system in the budding yeast, *Saccharomyces cerevisiae*. A single budding yeast E1, Uba1, initiates an intricate downstream ubiquitination network consisting of 11 E2s and 54 potential E3s that act on a multitude of proteins, marking them for destruction. At the apex of the entire pathway, the essential E1 gene, *UBA1*, is the logical target to disrupt all downstream ubiquitination reactions. Indeed, experiments conducted with a mouse cell line harboring a temperature-sensitive E1 provided the foundation for fundamental early discoveries on the nature of the UPS (Finley et al. 1984; Ciechanover et al. 1984; reviewed in Pickart and Cohen 2004). Yet, while conditional mutants of the *S. cerevisiae* E1 gene had previously been isolated, they only exhibit partial loss-of-function phenotypes, limiting their utility (Swanson and Hochstrasser 2000;

McGrath et al. 1991; Cheng et al. 2002). We reasoned that a strong, fast-acting, temperature-sensitive *uba1* mutant would be a valuable tool to address the role of ubiquitin conjugation in myriad processes. We show that it is possible to isolate such a mutant and, as a demonstration of its utility, we have used the *uba1-204* mutant to explore the nature of ubiquitin chain recognition and delivery pathways.

Phenotypic characterization of the *uba1-204* mutant revealed that it exhibited dramatic loss of both polyubiquitin conjugates and proteolysis at the restrictive temperature. Upon shifting mutant cells to 37°C, nearly all detectable ubiquitin conjugates disappeared in a matter of minutes, suggesting rapid inactivation of the mutant Uba1 protein. Moreover, the turnover of three proteins targeted by different ubiquitin ligases was severely inhibited in mutant cells held at the nonpermissive temperature. Together, the rapid loss of conjugates and the stabilization of three different UPS substrates suggest the interruption of multiple downstream proteolytic pathways. However, it is possible that there remains a level of ubiquitin activation sufficient to sustain some degradation pathways. Clb2 did not accumulate in G1-arrested *uba1-204* cells upon induction of its expression from a *GAL* promoter, whereas Clb2 lacking its destruction box did accumulate (A. Amon, personal communication). This observation suggests that APC-dependent degradation of Clb2 may continue despite the otherwise severe defects seen in *uba1-204*. It will be interesting in the future to determine the proteome-wide effects of this mutation.

To investigate the impact of polyubiquitin chain depletion on substrate delivery processes, we examined the ubiquitin-proteasome system at its terminus, the proteasome. We present evidence that while robust ubiquitination is not required for the maintenance of functional 26S proteasomes, it may regulate the recruitment of some ubiquitin binding proteins. In the absence of normal ubiquitination, Rpn10 incorporation into the

proteasome complex was unaltered. However, in extracts from *uba1-204* mutant cells, proteasomes were associated with reduced levels of the UbL/UBA proteins Rad23 and Dsk2.

Two models have been proposed to describe the mechanism of Rad23-mediated substrate delivery (reviewed in Madura 2004). According to the "shuttle factor" model, Rad23 first recognizes polyubiquitinated proteins via its UBA domains and subsequently shuttles substrates to the 26S proteasome. In contrast, the "alternative receptor" model predicts that Rad23 docks onto the proteasome via its UbL domain and acts alongside Rpn10 as a receptor for trapping polyubiquitinated substrates. Because they can be isolated largely free of associated ubiquitin chains, proteasomes from *uba1-204* cells provide a means of distinguishing between these two models by addressing the key question of whether Rad23 association with the proteasome depends on the availability of ubiquitinated substrates. A decrease in proteasome-bound Rad23 was observed in the *uba1-204* mutant. Moreover, the results in Figure 3-6 demonstrate that addition of polyubiquitin chains (either unanchored or substrate-bound) to a polyubiquitin-free *in vitro* system promoted Rad23 association with the proteasome. The defect in Rad23 targeting could also be rescued *in vivo* by increasing cellular polyubiquitin levels with the proteasome inhibitor MG132. Based on these results, we propose that the recognition of ubiquitin chains typically precedes (and activates) proteasomal targeting of Rad23. Conversely, if detection methods accurately reflect a near absence of ubiquitin conjugates in the mutant, then the remaining Rad23 residing on proteasomes isolated from these cells hints that Rad23 can operate as postulated by the alternative receptor model, albeit less efficiently than it functions as a shuttling factor.

Recent findings have suggested that intramolecular interactions can regulate Rad23 activity, resulting in a “closed conformation” and steric inhibition of the receptor. In hHR23a, the human homolog of Rad23, the UbL domain engages in a transient intramolecular interaction with both UBA domains (Walters et al. 2003). NMR spectroscopic analysis of yeast Rad23 has revealed that while the first UBA domain can participate in an intramolecular interaction with the UbL, the carboxy-terminal UBA domain does not (Kang et al. 2006). Intramolecular interactions could result in inhibition of intermolecular activity such as proteasome and ubiquitin chain binding. This may explain the finding that full-length Rad23 has a lower affinity for the proteasome than does its truncated UbL domain (Elsasser et al. 2002) and removal of the UbL domain from intact hHR23a increases its affinity for free Ub_6 chains four-fold (Raasi et al. 2004). These biophysical data predict that addition of ubiquitin conjugates should stimulate Rad23 association with ubiquitin-depleted proteasomes *in vitro*, and that depletion of ubiquitin conjugates *in vivo* should lead to reduced association of Rad23 with the proteasome, whereas accumulation of ubiquitin conjugates should enhance Rad23 association with the proteasome. All three of these predictions have been confirmed in this report. Taken together, the data suggest that in its “resting” state, Rad23 is in a closed conformation in which the UbL and first UBA domain engage in an intramolecular association. Upon coming into contact with substrate, the UBA domain preferentially binds the substrate’s ubiquitin chain owing to its ten-fold higher affinity for ubiquitin compared to UbL (Ryu et al. 2003). The exposed UbL domain can now bind to the proteasome. Although binding of Rad23’s UBA domains to polyubiquitin and its UbL domain to proteasome may be sequential, the process is not necessarily unidirectional. It is possible that disruption of the weak UbL-UBA intramolecular interaction could occur either through UBA recognition of a

polyubiquitin chain or through binding of UbL to proteasome, which could account for the presence of low amounts of Rad23 on proteasomes purified from *uba1-204* cells. Nevertheless, whether this binding is truly due to docking of "empty" receptor molecules or is merely an artifact of residual Uba1 activity, our data clearly demonstrate that ubiquitin chains significantly enhance stable association of Rad23 with the proteasome *in vitro* and *in vivo*.

In summary, we have isolated and characterized a new allele of budding yeast ubiquitin-activating enzyme that results in nearly complete inhibition of the ubiquitin-proteasome pathway. Our data reveal that while ongoing ubiquitination is not necessary for proteasome activity, ubiquitin conjugates promote the association of ubiquitin-binding substrate receptor proteins with the proteasome. In addition to regulated proteolysis, ubiquitin is involved in a broad range of other cellular functions, including cell-cycle control, transcription, DNA repair, signal transduction, and endocytosis. Mutant *uba1-204* cells will be a valuable tool in further exploration of ubiquitin-dependent proteolysis as well as the many other ubiquitin-dependent cellular processes.

MATERIALS AND METHODS

Yeast strain construction

To create the wild-type strain used in all experiments, a deletion of the *UBA1* gene was generated by a gene disruption technique described previously (Guthrie and Fink; 1991). *UBA1* was replaced by *Kanmx*, which was amplified by PCR using oligos

NG34

(5'AAAAAGTAAGATTAGTAGCAAAGCAAAGAACATATAACTATAGCTTCGACGTACGC TGCAGGTCGAC-3') and

NG37

(5'GGTTATAACGCATAGTGAACAAATGATGAGGTCTTGTAACTCGATTGCCATCGATG AATTCGAGCTCG-3'). Transformation of the resulting PCR product into W303 cells and selection for kanamycin resistance resulted in RJD3267, which contained a deletion of the entire coding sequence (as well as a partial deletion of the Ste6 gene, causing sterility in mating type a cells). The *UBA1* gene was amplified from wild-type W303 *S. cerevisiae* cells by PCR using oligos

NG19 (5'-CCGCTCGAGGGTAAAGTGGTTGAGCGAGGTA-3') and

NG20 (5'-GGACTAGTGAATTGCCATTACGCTTCC-3'; *Xho*I and *Spe*I sites underlined). The resulting PCR product, which contained *UBA1* coding sequences plus 186 bp upstream of the start codon and 269 bp downstream of the stop codon, was cloned into the CEN plasmid pRS316 to generate plasmid pRS316-UBA1. The diploid yeast strain RJD3267 was transformed with the pRS316-UBA1 plasmid, sporulation was induced, and a haploid strain was selected that contained both the deletion of *UBA1* and pRS316-UBA1 marked by *URA3*. A plasmid shuffling strategy was used to replace pRS316-UBA1 with pRS313-UBA1. The resulting strain, RJD3268, was used as the wild-type control strain in this study.

To generate mutant alleles of *UBA1*, random mutations were introduced into the *UBA1* gene by error-prone PCR using the GeneMorph Random Mutagenesis Kit (Stratagene, La Jolla, CA), NG19 and NG20 primers, and pRS316-UBA1 as the template. A gapped plasmid was created by digesting pRS313 with *Nhe*I. RJD3268 was

cotransformed with the mutagenized PCR product and the gapped pRS313 plasmid and transformants were plated onto –His media. Cells that had lost the *URA* plasmid carrying wild-type *UBA1* were selected by replica plating onto plates containing 5-fluoro-orotic acid incubated at 25°C. Fifty temperature-sensitive mutants were identified by screening for colonies that grew at 25 but not at 37°C.

Viability and stress sensitivity assay

Wild-type and *uba1-204* yeast cells were grown to an optical density of A_{600} = 1. Ten-fold serial dilutions were spotted onto YPD plates and SD plates containing 30 μM $CdCl_2$. All plates were incubated at the indicated temperatures for 2-3 days.

Flow cytometric analysis of DNA content

Cells were grown to log phase in YPD, washed, then incubated with 50 ng/ml α-factor for 2 hours at 25°C to arrest cells in G1 phase. For the experiment in Figure 1C, an additional 25 ng/ml α-factor was added and cultures were incubated at 37°C for 1hour. Cells were washed with YPD to reverse the α-factor arrest and resuspended in fresh YPD medium at 37°C. For the experiment in Figure 1D, an additional 25 ng/ml α-factor was added and cells were kept at 25°C for 1 hour. Cells were washed and grown in YPD at 25°C for 90 minutes to allow progression to G2 phase before shifting the cultures to 37°C.

Samples were withdrawn at indicated times after the shift to nonpermissive temperature, centrifuged at 13K rpm and resuspended in 70% ethanol for 1 hour at 4°C. The cell suspension was centrifuged for 5 minutes and washed with 50 mM sodium citrate. Cells were resuspended in 50 mM sodium citrate containing 0.25 mg/ml RNAse A and

incubated at 50°C for 1 hour. Cells were centrifuged and washed with phosphate-buffered saline pH 7.2. Proteinase K was added to 2 mg/ml and cells were incubated at 50°C for an additional hour. Propidium iodide was added at a final concentration of 16 μg/ml. Immediately prior to flow cytometric analysis, cells were sonicated twice at setting 3 for 3 seconds, and filtered with Tekto mesh screen into Falcon 2058 polystyrene tubes.

Extract preparation

Cells were harvested by centrifugation and frozen in liquid nitrogen. Cells were then resuspended in buffer containing 50 mM Tris (pH 7.5), 10% glycerol, 0.1% β-mercapto-ethanol, and 1% SDS. An equal volume of glass beads (Sigma, 425-600 μg, acid washed) was added and cell pellets were boiled for 3 minutes, vortexed in a ThermoSavant FastPrep for 45 seconds at a speed of 5.5, and boiled for an additional 2 minutes. Samples were resolved by SDS-PAGE, transferred to nitrocellulose, and probed with the indicated antibody. Antibodies were kindly provided by K. Madura (Robert Wood Johnson Medical School-UMDNY, Piscataway, NJ) for Rad23, M. Funakoshi (Kyushu University, Fukuoka, Japan) for Dsk2, R. Vierstra (University of Wisconsin-Madison, Madison, WI) for Rpn10, and J. Monaco (University of Cincinnati College of Medicine, Cincinnati, OH) for LMP.. Ubiquitin was detected with monoclonal antibody from Chemicon (Temecula, CA).

Deg1-GFP degradation

Cells harboring the Deg1-GFP plasmid (gift of R. Hampton) were grown in YP dextrose medium. Cultures of exponentially growing haploid yeast cells were incubated at

25°C or shifted to the nonpermissive temperature 37°C for one hour, and cycloheximide was added to 0.5 mg/ml. 5 ml aliquots were harvested every fifteen minutes and extracts were prepared as above and analyzed with antiserum to GFP (Clontech, Mountain View, CA). Strains used were RJD3272 (WT) and RJD3275 (*uba1-204).*

Ub^{V76}-V-βgal degradation

Cells harboring the *GAL-Ub^{V76}-V-βgal* plasmid (gift of A. Varshavsky) were grown in SC raffinose medium lacking uracil. *Ub^{V76}-V-βgal* expression was induced at the permissive temperature for 1 hour by the addition of galactose to 2%. Cultures were then incubated at either 25°C or shifted to 37°C for 1 hour and transferred to fresh medium containing 2% dextrose to extinguish synthesis of Ub^{V76}-V-βgal. Portions were withdrawn every 15 minutes and processed for immunoblotting with antiserum to β-galactosidase. Strains used were RJD3271 (WT) and RJD3274 (*uba1-204).*

Sic1 degradation

Cells grown in SC raffinose medium lacking uracil were arrested with α-factor (50 ng/ml) for 1 hour, and *GAL-SIC1* expression was induced transiently for 1 hour by the addition of galactose to 2%. Supplemental α-factor was added to 25 ng/ml when cells were shifted to 37°C for 1 hour. Cells were then washed and transferred to fresh medium containing 2% dextrose to quench *SIC1* expression, and portions were withdrawn every 30 minutes and processed for immunoblotting with antiserum to Sic1 (gift of L. Johnston, National Institute for Medical Research, London, United Kingdom). Strains used were RJD3270 (WT) and RJD3273 (*uba1-204).*

Native gel activity assay

26S proteasome samples were purified as described below and resolved by nondenaturing PAGE as described in Glickman et al. 1998. The gel was incubated with fluorogenic peptide Suc-LLVY-AMC for 10 minutes at 30 °C. Proteolytic activity of the resolved complexes was visualized by exposure to UV light. Protein complexes in the same gel were also detected with Coomassie blue stain.

In vitro Ub-Sic1 degradation

Ub-Sic1 was synthesized as described in Saeki et al. 2005. 0.5 μM Ub-Sic1 was incubated with 1 μM 26S proteasome in the presence of 3 mM Magnesium acetate and 1X ARS (Verma et al. 1997) for 0 or 5 minutes as specified. Proteasomes treated with 100 μM epoxomicin were pre-incubated with drug at 30°C for 30 minutes prior to addition of Ub-Sic1. Reactions were terminated by adding SDS Laemmli buffer and samples were resolved by SDS-PAGE, blotted to nitrocellulose, and visualized with antibody to Sic1 (gift of L. Johnston).

Preparation of extracts for affinity purification of 26S proteasomes

Yeast strains RJD3276 (WT) and RJD3277 (*uba1-204)* were grown to log phase at 25°C in medium containing 0.67% yeast nitrogen base minus amino acids, 2% dextrose, 0.5% casamino acids, and 20 mg/l adenine and tryptophan. Cultures were split in half and 25°C cultures were incubated for 40 minutes at 25°C, while 37°C cultures were pelleted by centrifugation, resuspended in fresh 37°C medium, and incubated at 37°C for 40 minutes. Cells were pelleted by centrifugation for 5 minutes at 4°C for 25°C samples and at 37°C for

37°C samples. Pellets were washed with 25°C or 37°C sterile water and frozen in liquid nitrogen for a minimum of 2 hours. Frozen cell pellets were ground to a fine powder under liquid nitrogen in a mortar placed on a bed of dry ice. Powder was resuspended in one pellet-volume of column buffer containing 50 mM Tris, pH 7.5, 150 mM NaCl, 10% glycerol, 5 mM $MgCl_2$, 5 mM ATP. ATP Regenerating System (ARS) (Verma et al. 1997) was added and the lysates were clarified by centrifugation at 17,000 rpm for 20 minutes.

Lysates were supplemented again with 5 mM ATP and 5 mM $MgCl_2$ and incubated at 4°C for 2 hours with FLAG antibody-coupled beads from Sigma (St. Louis, MO) that had been pre-washed in 0.1 M glycine, pH3.5 and resuspended as a 50% slurry with column buffer. For each sample, 1.5 ml of lysate was incubated with 1 ml bead slurry. Bead-bound proteins were pelleted and washed three times with high salt wash buffer consisting of the column buffer described above supplemented with 0.2% Triton X-100 and NaCl to a final concentration of 200 mM.

For Coomassie blue staining, immunoprecipitations, and native gel experiments, bead-bound proteins were then washed twice with low-salt wash buffer containing 50 mM Tris-HCl, pH7.5, 20 mM $MgCl_2$, 2 mM ATP. All supernatant was aspirated with a 25 gauge needle, and the pellet was resuspended in three times its volume of elution buffer containing 25 mM Tris, pH7.5, 150 mM NaCl, 5 mM $MgCl_2$, 2 mM ATP, and 100 μg/ml Flag peptide and proteins were eluted at 4°C for 3 hours. Samples were analyzed by SDS-PAGE on a 4%-12% Tris-Glycine gel (Invitrogen, Carlsbad, CA).

For proteasome binding experiments in Figure 6A-C, bead-bound proteasome complexes were resuspended in column buffer and incubated with 1 mM phenanthroline, 2.5 μM ubiquitin-aldehyde (Boston Biochem., Cambridge, MA), 100 μM MG132, 1 mM ATP, and 5 mM $MgCl_2$ on ice for 1 hour. Purified proteins were added as indicated and

samples were incubated on ice for 1 hour. GST-Rad23, GST-UbL, GST-UBA, and Rad23-HIS were gifts from R. Verma (Caltech), Sic1 was a gift from G. Kleiger (Caltech), and Ub_4 was from Boston Biochem. (Cambridge, MA). The bound fraction was washed three times with high salt wash buffer, twice with low salt wash buffer, supernatant was aspirated, and proteins were eluted with SDS loading buffer and analyzed by SDS-PAGE on a gradient gel.

MG132 binding assay

Yeast strains that were sensitive to proteasome inhibitors were generated by deletion of the *pdr5* gene. RJD3983 (WT) and RJD3984 (*uba1-204*) were grown in casamino acids medium at 25°C and MG132 (American Peptide, Sunnyvale, CA) or DMSO was added. After five minutes 37°C medium was added to shift cells to the nonpermissive temperature and cultures were incubated at 37°C for 1 hour. Cells were centrifuged at 37°C for five minutes and flash frozen. 26S proteasome complexes were purified as described above.

Chapter 4

QUANTITATIVE MASS SPECTROMETRIC ANALYSIS OF AFFINITY PURIFIED 26S PROTEASOME COMPLEXES

INTRODUCTION

Ubiquitin-dependent proteolysis is the major non-lysosomal pathway of protein degradation in eukaryotic cells. While regulation of the enzymatic cascade responsible for polyubiquitination of proteins has been thoroughly studied, the mechanisms involved in recognition and delivery of ubiquitinated substrates to the proteasome remain unclear. Recent work has shown that a diverse set of ubiquitin-binding receptors function to control the targeting of ubiquitinated proteins to the proteasome in a substrate-specific manner (Chen and Madura 2002; Elsasser et al. 2004; Verma et al. 2004; Wilkinson et al. 2001; reviewed in Elsasser and Finley 2005; Hicke et al. 2005).

Recent developments in mass spectrometry technology have enabled proteomic analysis of ubiquitinated proteins and their interaction with the proteasome (reviewed in Xu and Peng 2006). Large-scale analysis of His_6-ubiquitinated peptides by mass spectrometry uncovered 1075 putative ubiquitinated proteins (Peng et al. 2003). Work done in our laboratory coupled the one-step affinity purification of intact proteasome complexes with mass spectrometry to create a new approach to analyzing the "interactome" of the proteasome (Verma et al. 2004). The success of these large-scale proteomic analyses lead to further investigation of the ubiquitin-proteasome pathway using genetic mutants to profile specific ubiquitination pathways. Hitchcock et al. (2003) used

this approach to identify a set of membrane-associated substrates of the endoplasmic reticulum associated degradation (ERAD) pathway and Mayor et al. (2005) identified ubiquitinated proteins that are selectively accumulated in rpn10Δ cells.

Multidimensional Protein Identification Technology (MudPIT) is a recent strategy that uses "shotgun proteomics" (Wolters et al. 2001), separating proteins that have been digested into peptides rather than intact proteins. This allows analysis of complex protein mixtures by capillary chromatographic separation of peptides. Once the peptide mixture is loaded onto the column, the column is placed in-line with an electrospray-ionization ion-trap tandem mass spectrometer (Link et al. 1999; Washburn et al. 2002; Wolters et al. 2001). Acquired fragmentation spectra are matched to translated genomic sequence data via Sequest (Eng et al. 1994). MudPIT has been successfully used in our laboratory to study the *S. cerevisiae* ubiquitin-proteasome system (Verma et al. 2004; Mayor et al. 2005, Graumann et al. 2004), and its implementation is discussed in detail in the dissertation of Johannes Graumann (2006).

Our recent characterization of a genetic mutant strain in which ubiquitin remains inactive, inert, and unable to label proteins for degradation by the proteasome provides a unique cellular environment for mass spectrometric analysis. We have demonstrated that in *uba1-204* cells, proteasome complexes remain intact and active, but do not encounter ubiquitinated substrates (Ghaboosi and Deshaies 2007). In addition, these proteasomes associate with lower levels of the ubiquitin-binding proteins Rad23 and Dsk2. In this study, we analyze proteasome complexes isolated from wild-type and *uba1-204* mutant cells using MudPIT in order to determine the affect of cellular depletion of ubiquitin chains on the association of proteins with the proteasome. This work was done in collaboration with

Johannes Graumann, Thibault Mayor, and Geoff Smith, who conducted LC/MS/MS analysis of peptide samples which I prepared. While this is a preliminary study and the findings described here have yet to be validated, this work does highlight the potential value of this novel ubiquitin pathway mutant in systematic analysis of the ubiquitin-proteasome pathway.

RESULTS

MudPIT analysis of metabolically labeled proteasome complexes

Having established a unique cellular environment in which proteasome complexes were presented with severely reduced levels of ubiquitinated substrates and ubiquitin-binding proteins Rad23 and Dsk2, we next tested the feasibility of using MudPIT to determine the proteomic affect on the proteasome complex. In order to create protein populations *in vivo* that are distinguishable by mass spectrometry, cell cultures were grown in conditions that would create metabolically labeled proteins (Oda et al. 1999; MacCoss et al. 2003). Wild-type and *uba1-204* cells were grown in minimal media supplemented with a "heavy" ^{15}N nitrogen source or a "light" ^{14}N nitrogen source, respectively, in the form of ammonium acetate. Thus, proteins formed in each strain were uniformly labeled with peptides displaying a discernible mass shift. The technique of metabolic labeling also allows preparation and analysis of samples to be done simultaneously rather than in parallel. Wild-type and *uba1-204* cells are mixed, lysed, separated in the same column,

and analyzed simultaneously, reducing any potential discrepancies due to errors in experimental reproducibility.

First, strains were generated which could be grown in minimal media. Wild-type (RJD3983) and *uba1-204* (RJD3984) strains were grown in different growth conditions in order to label proteins from each strain with “heavy” or “light” nutrients. Cultures were shifted to the nonpermissive temperature for twenty minutes, and proteasome complexes were affinity purified as described in materials and methods. Affinity purified proteins from wild-type and *uba1-204* cells were mixed and digested. The peptide mixture was delivered to Johannes Graumann who, in conjunction with Thibault Mayor and Geoff Smith, analyzed the samples by multidimensional LC-MS/MS, or MudPIT. The spectra generated were evaluated using algorithms from Sequest (Eng et al. 1994) and DTASelect/Contrast (Tabb et al. 2002) and quantification software RelEx (MacCoss et al. 2003) was used to generate comparative results.

By coupling the affinity purification of intact proteasome complexes with quantitative mass spectrometry, we were able to identify a total of 383 proteins, including all subunits of the proteasome. Comparative quantitation of labeled peptides yielded 234 proteins that had unaltered levels in mutant cells, 60 proteins that were depleted in proteasomes isolated from *uba1-204* cells, and 89 proteins that were enriched in the *uba1-204* proteasome sample (Figure 4-1).

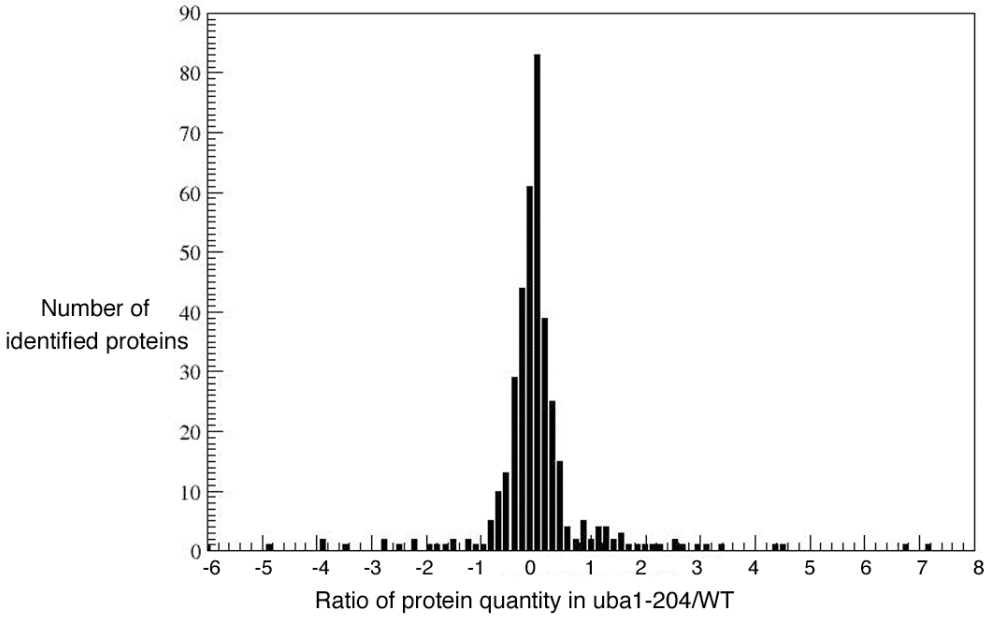

Figure 4-1. Distribution of ratio of ^{14}N-labeled peptides from *uba1-204* cells / ^{15}N-labeled peptides from wild-type cells.

Proteasome-associated proteins with unaltered levels in uba1-204

Of the proteins that were quantified at similar levels in wild-type and mutant cells, all subunits of the proteasome were observed (Figure 4-2). This result was confirmed experimentally by resolving affinity purified proteasome complexes by SDS-PAGE and visualizing subunits by Coomassie blue staining (Figure 3-4A).

Gene	204/WT	SD	Peptides
SDS23	-3.341	5.989	2
DNM1	-2.375	2.762	2
END3	-2.207	3.223	2
YLR199C	-2.182	2.25	2
RPL21A	-1.841	2.132	2
NOG2	-1.599	2.201	2
YPK2	-0.813	1.413	2
RRP5	-0.714	0.982	5
RVB1	-0.67	1.575	2
SSA1	-0.634	1.285	6
FAS1	-0.626	0.84	6
RPL16B	-0.611	1.283	3
RPL20A	-0.548	0.656	5
CDC39	-0.475	0.532	5
SLA2	-0.457	0.712	2
ARO1	-0.45	0.56	10
ADE16	-0.449	0.75	4
GLT1	-0.444	0.654	4
RPL1B	-0.422	0.896	3
FAS2	-0.4	0.55	3
CDC33	-0.399	0.481	5
GPD1	-0.394	0.421	19
RPL14B	-0.393	1.371	5
ABP1	-0.384	0.993	4
HIS4	-0.379	0.522	3
MET17	-0.355	0.636	4
NUP82	-0.351	0.54	2
YDR098C-B	-0.349	1.621	2
NUG1	-0.344	0.347	7
YKL206C	-0.325	0.35	5
RPS11B	-0.32	0.393	4
STU2	-0.319	0.405	4
TUB2	-0.317	0.529	2
RRP6	-0.31	1.24	4
CYS4	-0.305	1.874	3
RPL17B	-0.302	1.204	3
TDH3	-0.265	0.61	6
LSP1	-0.259	0.608	5
SRV2	-0.248	0.583	2
ECM17	-0.245	0.311	5
DBP3	-0.227	0.651	2
ADE17	-0.223	0.32	6
COQ1	-0.217	0.269	4
BMH2	-0.216	0.353	11
RPL27B	-0.212	0.29	3
RPS6B	-0.212	0.394	7
LYS20	-0.204	0.204	7
TPD3	-0.203	0.517	2
TSA1	-0.201	0.252	4

Gene	204/WT	SD	Peptides
HSP60	-0.197	0.24	12
CCT3	-0.186	0.751	5
RPL10	-0.179	0.356	13
ARF1	-0.176	0.503	2
CLA4	-0.174	1.483	3
SER1	-0.174	0.419	17
THI20	-0.171	0.325	20
CDC48	-0.169	0.561	7
RPL4A	-0.165	0.512	8
LEU2	-0.163	0.279	12
FUN12	-0.16	2.021	3
RPS0A	-0.16	0.807	4
ECM29	-0.158	0.372	3
URA2	-0.151	0.365	7
PFK1	-0.147	0.531	11
RPS4B	-0.143	0.216	5
PRE8	-0.14	0.187	46
CCT6	-0.139	0.406	6
PIH1	-0.137	0.266	2
BMH1	-0.119	0.372	13
RPS10B	-0.119	0.583	4
NOP58	-0.117	0.343	3
HIS5	-0.116	0.135	5
RPL12B	-0.115	0.339	3
RPL8B	-0.112	0.188	15
RPN5	-0.106	0.39	9
TDH1	-0.105	0.239	4
TUF1	-0.105	0.335	4
RPL7A	-0.102	0.193	6
CCT2	-0.099	0.422	9
RRP3	-0.098	0.126	3
PRE10	-0.096	0.167	47
LYS21	-0.094	0.37	8
PRE7	-0.093	0.206	40
RPL35B	-0.093	0.326	4
CDC19	-0.091	0.157	40
PRE6	-0.088	0.19	66
YOR220W	-0.084	0.336	3
RPS7A	-0.081	0.102	6
RPL2A	-0.078	0.437	10
SCL1	-0.074	0.169	88
ZPR1	-0.074	0.392	3
RPN11	-0.069	0.294	24
VMA2	-0.067	0.411	6
ILV1	-0.064	0.238	11
SUP35	-0.064	0.283	4
YKT6	-0.058	0.333	7
ENO1	-0.048	0.216	6
RPS31	-0.048	0.276	3

Gene	204/WT	SD	Peptides
SCP160	-0.047	0.177	7
PRE5	-0.043	0.194	58
PUP3	-0.041	0.189	29
CSR1	-0.041	0.411	6
YBR025C	-0.037	0.233	11
BLM3	-0.022	0.852	6
RPS1B	-0.021	0.316	12
RPS25A	-0.016	0.279	3
PRE2	-0.015	0.226	49
TCP1	-0.013	0.505	3
TEF2	-0.012	0.197	49
RPS12	-0.005	0.498	3
ILV6	0.003	0.215	5
GFA1	0.004	0.157	13
ILV2	0.006	0.266	8
SUB2	0.012	0.502	7
VMA5	0.014	0.495	9
PRE1	0.016	0.092	21
SYP1	0.016	0.166	5
PUP2	0.018	0.314	55
PUP1	0.02	0.164	25
HSC82	0.023	0.272	88
RPS1A	0.023	0.141	13
RPN13	0.026	0.172	17
HOG1	0.028	0.219	5
LYS12	0.032	0.139	23
RPS20	0.035	0.388	8
CCT4	0.035	0.158	6
MET6	0.037	0.247	10
PRE4	0.037	0.28	30
RPL9A	0.04	0.082	5
PRE3	0.042	0.482	44
RPS3	0.042	0.183	5
SSB1	0.043	0.488	2
GDH1	0.044	0.614	4
ATP1	0.046	0.294	4
HOM3	0.046	0.419	3
CCT7	0.047	0.197	2
PDC1	0.05	0.359	20
PUF4	0.051	0.352	3
RPS18A	0.052	0.31	9
TIF2	0.052	0.474	14
RPN10	0.053	0.175	20
RPL23A	0.058	0.269	8
SRO9	0.062	0.258	3
ACC1	0.063	0.526	18
MET16	0.067	0.074	2
RPL28	0.067	0.141	4
RPS5	0.07	0.388	8

Gene	204/WT	SD	Peptides
RPS2	0.071	0.11	6
RPL16A	0.072	0.508	4
ARG5,6	0.074	0.196	10
PGI1	0.074	0.578	2
PRE9	0.076	0.281	48
RPN1	0.08	0.22	107
VMA8	0.08	1.177	6
RPL19B	0.081	0.126	8
GPM1	0.082	0.251	13
PGK1	0.086	0.489	10
RPA190	0.086	0.304	2
EFT2	0.089	0.304	20
RPN8	0.09	0.183	59
RPS22A	0.092	0.269	2
RPT2	0.092	0.212	63
RPT4	0.095	0.33	40
TIF35	0.098	0.897	2
TRP5	0.098	0.31	43
ARO8	0.099	0.42	3
RPL4B	0.099	0.195	7
YOR112W	0.1	0.229	5
RPT1	0.102	0.304	43
CDC9	0.106	0.407	4
NOP1	0.107	0.952	3
RPT5	0.114	0.443	64
CCT5	0.116	0.64	4
RPP0	0.119	0.148	6
YEF3	0.129	0.54	10
RPN6	0.131	0.145	50
RPT3	0.131	0.26	54
DBP5	0.132	0.686	6
RPN7	0.133	0.178	22
LEU1	0.138	0.343	8
TDH2	0.139	0.205	9
ENO2	0.143	0.88	14
RPS24A	0.144	0.319	6
RPN2	0.156	0.287	69
CCT8	0.161	0.401	5
ARB1	0.164	0.326	6
RPN3	0.165	0.543	15
RPG1	0.17	0.204	6
RPL6A	0.174	0.224	2
RPT6	0.175	0.319	45
SDS24	0.175	0.594	12
GCN1	0.176	0.447	7
SSA4	0.217	0.423	5
ACT1	0.22	0.485	5
MOT1	0.226	0.636	2
SUA7	0.229	1.324	2

Gene	204/WT	SD	Peptides
MET10	0.241	0.355	2
NEW1	0.245	0.522	6
PFK2	0.245	0.292	2
TIF34	0.252	0.399	2
YPK1	0.266	0.727	5
RPL15A	0.271	0.992	3
ALD3	0.282	0.401	6
MET13	0.297	0.367	2
TWF1	0.297	0.397	6
RPL30	0.309	0.9	3
RPL17B	0.315	0.488	2
TIF4631	0.321	0.467	5
RPS17B	0.324	0.621	3
SRP1	0.328	0.364	10
RPL38	0.336	0.563	4
PIM1	0.345	1.41	2
SSB2	0.346	0.755	5
SAM1	0.351	0.499	16
ALD6	0.359	0.689	4

Figure 4-2. List of proteins with unaltered abundance in *uba1-204* proteasomes. List of identified proteins for which quantitative analysis showed unaltered peptide levels in *uba1-204* and wild-type samples. "204/WT" reflects the ratio of $^{14}N/^{15}N$ isotope-labeled peptides, "SD" lists the standard deviation, and "peptides" is the number of peptides identified for each protein.

Unfortunately, although Rad23 has been identified in previous mass spectrometry experiments, we were unable to determine the presence of either Rad23 or Dsk2 in our proteomic analysis. This is likely due to the low levels of these substoichiometric proteins present at the proteasome. However, we did recover some proteins that are known to be involved in the ubiquitin-proteasome pathway, including Cdc48, which was identified by 7 peptides at quantitative levels that were unaltered in the mutant. Indeed, we had

experimentally observed that, unlike Rad23 and Dsk2, the amount of Cdc48 associated with the proteasome was not affected in *uba1-204* cells (Figure 4-3).

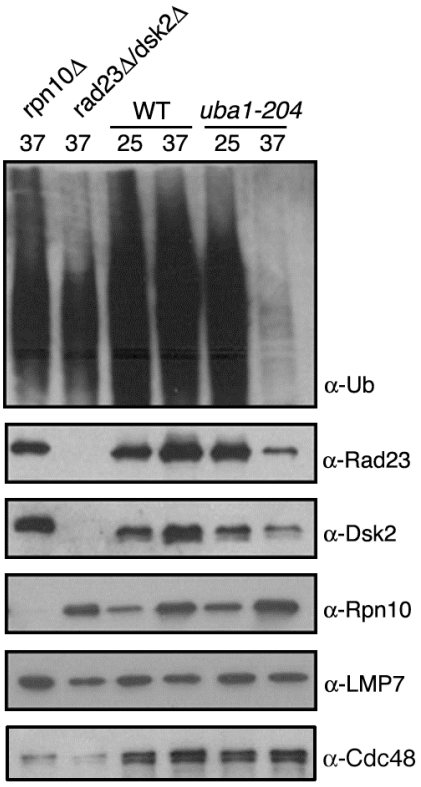

Figure 4-3. Cdc48 association with the proteasome is unaffected in *uba1-204* cells. Wild-type and *uba1-204* cells expressing Pre1-FH were grown in casamino acid medium and half the cultures were shifted to 37°C for 40 minutes. Lysates were prepared and immunoprecipitated as described in materials and methods by incubation with anti-Flag resin in the presence of ATP. Intact 26S proteasomes were eluted with Flag peptide, separated by SDS-PAGE, and proteasome-bound proteins were detected by immunoblotting with antiserum to the specified proteins.

Proteasome-associated proteins with depleted levels in uba1-204

Due to the large amount of information obtained from a single MudPIT experiment, we focused our attention on the relatively small number of proteins that displayed altered association with proteasomes purified from *uba1-204* cells. Proteins which are more abundant at the proteasome, including stoichiometric components such as subunits, will be represented by more identified peptides. While multiple peptide hits increases the confidence in the abundance calculation, proteins that have been identified by a single peptide may also yield important results. To uncover proteins that would be present at extremely low levels, such as ubiquitinated substrates, proteins identified by a single peptide were included. In multiple tandem mass spectrometric analyses of the soluble portion of the *S. cerevisiae* proteome, it was found that even proteins identified by single peptide hits generally resulted in accurate relative abundance calculations (Washburn et al. 2002). Comparing our results to several other large-scale proteomic studies of ubiquitinated proteins confers an additional level of confidence to the data. However, results obtained from this study, especially those based upon quantitation of a single peptide, should be verified by multiple mass spectrometric analyses or by biochemical means.

Having established that these proteasome complexes bind to significantly lower levels of ubiquitin chains (Figure 3-5A) and that substrates are not degraded by these proteasomes *in vivo* (Figure 3-3), we anticipated a decrease in the levels of known ubiquitin-proteasome pathway substrates in the labeled peptides purified from mutant proteasomes. Half of the proteins identified in this study as having the greatest decrease

in peptide levels in the mutant sample (and therefore a low 204/WT ratio) have also been identified as ubiquitinated proteins in multiple other screens (Peng et al. 2003; Hitchcock et al. 2003; Mayor et al. 2005; Verma et al. 2004) (Figure 4-4, right column).

Gene	204/WT	SD	Peptides	Gene Product	Ub
ADE12	-5.966	0	1	Adenylosuccinate synthetase, carries out addition of asp to IMP with GTP hydrolysis	
GVP36	-4.878	0	1	Cytoplasmic protein with possible role in cell-cycle regulation	b, c
SEC23	-3.869	0.551	3	Component of COPII coat of vesicles, ER to Golgi transport, GAP activity for Sar1p	
RGD2	-3.816	0	1	Unknown, GTPase activating protein (GAP) on both Cdc42p and Rho5p	
VMA13	-2.741	2.606	2	Vacuolar H(+)-ATPase, required for V-ATPase activity	a, b
HSF1	-2.658	0.047	2	Heat shock tf that binds to the heat shock DNA element at both normal and elevated temp	a
CDC10	-1.742	1.433	2	Septin, component of 10 nm filaments of mother-bud neck, involved in cytokinesis	
SAR1	-1.407	0	1	Component of COPII coat of vesicles, ER to Golgi transport, GTP-binding protein of the arf family in the ras superfamily	
HPT1	-1.381	0	1	Hypoxanthine-guanine phosphoribosyl transferase	a
NIP1	-1.208	0	1	Subunit of translation initiation complex eIF3, also required for nuclear import	a
HHF1	-1.155	0	1	Histone H4, identical to Hhf2p	
BBC1	-1.08	0	1	Protein involved in the regulation of myosin function and the actin cytoskeleton, interacts with Myo3p and Myo5p	
PMA1	-0.801	0.458	4	H+-transporting P-type ATPase of the plasma membrane required for nutrient uptake and pH homeostasis	a, b, c
PAB1	-0.776	0.748	2	Poly(A)-binding protein of cyt and nucleus, part of the 3'-end RNA-processing complex, translation termination with Sup35p	b
MCM6	-0.767	0.357	2	Protein involved in DNA replication, member of the MCM/P1 family of proteins	b
SEC21	-0.673	0.739	1	Coatomer (COPI) complex gamma chain of secretory pathway vesicles, required for retrograde Golgi to ER transport	a
GCD6	-0.651	0	1	Translation initiation factor eIF2B (guanine nucleotide exchange factor), 81 kDa (epsilon) subunit	a
VMA4	-0.604	0	3	Vacuolar H(+)-ATPase (V-ATPase) hydrophilic subunit (subunit E), 27 kDa subunit of V1 sector	
SIK1	-0.591	0.186	4	Nucleolar protein component of box C/D snoRNPs,component of the 80S U3 snoRNA complex,required for nucleolus morphology	

Gene	204/WT	SD	Peptides	Gene Product	Ub
NOG1	-0.563	0.498	1	Putative essential nucleolar GTP-binding protein, required for large ribosomal subunit biogenesis and export from the nucleolus	
YER139C	-0.525	0	1	Unknown	
SEC26	-0.458	0	1	Coatomer (COPI) complex beta chain of secretory pathway vesicles, required for retrograde transport from Golgi to ER	
MAE1	-0.454	0	3	Mitochondrial malic enzyme, (S)-malate:NAD(P)+ oxidoreductase (decarboxylating)	
KAP123	-0.452	0.258	11	Karyopherin-beta involved in nuclear import of ribosomal proteins	a, c
ALD4	-0.432	0.347	1	Mitochondrial aldehyde dehydrogenase	
GCD7	-0.415	0	1	Translation initiation factor eIF2B (guanine nucleotide exchange factor), 43 kDa subunit	a
PBS2	-0.407	0	3	MAP kinase kinase activated by high osmolarity through the Sln1p-Ypd1p-Ssk1p two-component and the Sho1p osmosensor	
ATP2	-0.388	0.049	2	Beta subunit of the F1 subunit of ATP synthase-mitochondrial respiratory complex V	
SEC18	-0.381	0.011	4	Required for fusion of vesicles to target membranes and for vacuolar fusion, member of the AAA family of ATPases	
RPP1A	-0.355	0.108	1	N-terminally acetylated protein component of the large (60S) ribosomal subunit	
SPT5	-0.351	0	1	Component of the SAGA complex and the SLIK (SAGA-like) complex, member of TBP (TATA-binding protein) class of SPT proteins	
TUB3	-0.34	0	1	Tubulin alpha-3 chain, non-essential	
AHA1	-0.336	0	7	Co-chaperone that activates Hsp82p ATPase activity	a
POL1	-0.333	0.158	1	DNA polymerase I alpha 180 kDa subunit	a
CLU1	-0.327	0	1	Translation initiation factor eIF3, p135 subunit	a
NOP14	-0.322	0	1	Nuclear and nucleolar protein, 40S ribosomal subunit biogenesis and 18S rRNA maturation, component of 80S U3 snoRNA complex	a
URA7	-0.294	0	2	CTP synthase, catalyzes the final step in the pyrimidine biosynthesis pathway	a
SAM2	-0.281	0.06	8	S-adenosylmethionine synthetase 2	a
FES1	-0.25	0.14	3	Nucleotide exchange factor for the cytosolic chaperone Ssa1p, involved in protein synthesis and resistance to H2O2	a
RPL8A	-0.245	0.185	4	Ribosomal protein L8, involved in maintenance of M1 dsRNA virus	a, c

Gene	204/WT	SD	Peptides	Gene Product	Ub
MET7	-0.243	0.214	1	Folylpolyglutamate synthetase, involved in methionine biosynthesis and maintenance of mitochondrial genome	
WTM1	-0.233	0	1	Transcriptional modulator involved in meiotic regulation and silencing	
YOD1	-0.231	0	1	Possible DUB, member of the ovarian tumor (OTU)-like cysteine protease family	a
ATG20	-0.218	0	1	Endosomal protein involved in retrograde transport	
CDC73	-0.216	0	1	RNA polymerase II accessory protein, may be involved in transcription elongation	
DHH1	-0.215	0	4	Putative RNA helicase required for normal sporulation, member of the DEAD/DEAH-box RNA helicase family	a, d
TPS2	-0.183	0.092	1	Trehalose-6-phosphate phosphatase, component of the trehalose-6-phosphatase synthase/phosphatase complex	a
GLY1	-0.171	0	1	Threonine aldolase, required for glycine biosynthesis	a, b, d
RBG2	-0.155	0	1	Unknown, similarity to mammalian developmentally regulated GTP-binding protein	
KIN1	-0.142	0	1	Serine/threonine protein kinase, related to Kin2p	
RPL11B	-0.125	0	1	Ribosomal protein L11	c
CHD1	-0.111	0	1	Protein involved in ATP-dependent nucleosome remodeling and DNA replication-independent nucleosome assembly, CHD family	a
UBX4	-0.075	0	2	Protein involved in tetrad formation, contains the UBX (ubiquitin-regulatory) domain	
NOB1	-0.062	0.017	1	Essential protein that functions in 20S proteasome maturation and 26S assembly, component of pre-40S ribosomal particle	
RPL31A	-0.059	0	1	Protein component of the large (60S) ribosomal subunit	
RPS14A	-0.053	0	5	Ribosomal protein S14A, involved in cryptopleurine resistance	d
YPR118W	-0.042	0.022	1	Methylthioribose-1-phosphate isomerase related to regulatory eIF2B subunits	
ADE13	-0.039	0	1	Adenylosuccinate lyase, carries out the eighth step in de novo purine biosynthesis	a
RPL26B	-0.038	0	1	Ribosomal protein L26	
RPL40A	-0.025	0	1	Fusion protein whose N-terminal half is ubiquitin and whose C-terminal half is ribosomal protein L40	c, d

Figure 4-4. List of proteins depleted in *uba1-204* proteasomes. List of genes identified as depleted in *uba1-204* affinity purified 26S proteasome sample compared to wild-type sample. "204/WT" reflects the ratio of $^{14}N/^{15}N$ isotope-labeled peptides, "SD" lists the standard deviation, and "peptides" is the number

of peptides identified for each protein. The column entitled “Ub” denotes proteins which have been identified in the following published mass spectrometry experiments: (a) Peng et al. 2003; (b) Hitchcock et al. 2003; (c) Mayor et al. 2005; (d) Verma et al. 2004.

In addition to the identification of proteins shown to be ubiquitinated in previous mass spectrometric analyses, we also identified proteins that had been experimentally proven to be substrates of the ubiquitin-proteasome pathway. Sec23, a component of the COPII coat vesicle essential for transport between the endoplasmic reticulum and Golgi, was identified by multiple peptides at levels that were significantly decreased in the *uba1-204* sample, suggesting that it may be a ubiquitinated substrate of the proteasome (Figure 4-4). Indeed, it has been shown that formation of the COPII complex is regulated by the ubiquitination and degradation of Sec23 (Cohen et al. 2003). Interestingly, all subunits of the COPII complex and its regulators were identified in this screen, including Sec24, Sec13, Sec31 (Figure 4-5). In addition, its regulators Sar1, and Arf1 and the deubiquitination complex Bre5 and Ubp3 were also identified (Figure 4-2, 4-4).

Proteasome-associated proteins with enhanced levels in uba1-204

Gene	204/WT	SD	Peptides	Gene Product	Ub
CIC1	7.223	0	1	Protein associated with the 26S proteasome, may be involved in regulated degradation of F-box proteins Cdc4p and Grr1p	
TRP3	6.782	0	1	Anthranilate synthase:indole-3-glycerol phosphate synthase, involved in the tryptophan biosynthesis pathway	a
ILV5	4.511	0	1	Ketol-acid reductoisomerase, involved in valine and isoleucine synthesis	
YIL110W	4.384	0	1	Unknown, predicted function in RNA processing	
THR1	3.422	0	1	Homoserine kinase (ATP:L-homoserine-O-P-transferase), first step in the threonine biosynthesis pathway	
CPA2	3.141	0	1	Carbamoylphosphate synthetase of arginine biosynthetic pathway	a
SER3	2.975	0	1	3-phosphoglycerate dehydrogenase, catalyzes the first step in synthesis of serine from 3-phosphoglycerate	a
SSC1	2.771	0	1	Mitochondrial heat-Mitochondrial protein that acts as an import motor with Tim44p and as a chaperonin in receiving and folding protein chains during import, protects mitochondrial DNA synthesis activity (Mip1p) during heat shock, heat shock protein of HSP70 family shock protein, member of the HSP70 family	
RPL6B	2.662	0	1	Protein component of the large (60S) ribosomal subunit	c
SEC24	2.333	1.082	2	Component of the COPII coat of vesicles, involved in endoplasmic reticulum to Golgi transport	a
RPL18B	2.209	0	1	Protein component of the large (60S) ribosomal subunit	c
PSA1	2.053	0	1	Mannose-1-phosphate guanyltransferase, GDP-mannose pyrophosphorylase	
RSC8	1.841	0	1	Component of abundant chromatin remodeling complex (RSC)	
SDH1	1.658	0.151	2	Succinate dehydrogenase (ubiquinone) flavoprotein (Fp) subunit, converts succinate plus ubiquinone to fumarate plus ubiquinol in the TCA cycle	
RFC1	1.566	0	1	DNA replication protein RFC large subunit	c
RPC40	1.541	0	1	Shared subunit of RNA polymerases I and III	
RPS9B	1.354	1.33	3	Ribosomal protein S9	a
PDR16	1.314	0.837	2	Phosphatidylinositol transfer protein, involved in lipid biosynthesis and multidrug resistance	
CDC47	1.235	1.047	2	Member of MCM/P1 family of proteins involved in DNA synthesis initiation, also regulates its own transcription	
BAT1	1.181	0	1	Mitochondrial branched-chain amino acid transaminase	

Gene	204/WT	SD	Peptides	Gene Product	Ub
SSZ1	1.019	0	1	Pleiotropic drug resistance protein, associates with Zuo1p to form the ribosome-associated complex, member of the Hsp70 family	
CBF5	1.005	0.287	2	Ribosomal RNA pseudouridine synthase, associated with H/ACA class small nucleolar RNAs	a, c
TIF4632	0.903	0.141	2	Translation initiation factor eIF4G, subunit of the mRNA cap-binding protein complex (eIF4F) that also contains eIF4E (Cdc33p)	
TAF5	0.893	0	1	Component of the TAF(II) complex (TBP-associated protein complex) and SAGA complex, required for activated transcription by RNA polymerase II	*
STH1	0.864	0	1	Component of abundant chromatin remodeling complex (RSC), involved in the response to DNA damage	a
CCR4	0.806	0.543	4	Component of the CCR4 transcriptional complex and catalytic component of the major cytoplasmic mRNA deadenylase with 3'-5' exonuclease activity	
NUM1	0.79	0	1	Nuclear migration protein, controls interaction of bud-neck cytoskeleton with G2 nucleus	b, c
YSC84	0.696	0.691	2	Protein involved in cortical actin patch polarization with Lsb5p, also involved in fluid phase endocytosis and vesicle trafficking	
YBR012W-B	0.623	0.068	3	Transposable element gene	
RPL14B	0.593	0.557	3	Ribosomal protein L14	
MCK1	0.576	0	1	Member of the GSK3 subfamily of protein kinases, positive regulator of meiosis and spore formation	a
RVS167	0.569	0	1	Protein that affects actin distribution and bipolar budding	a, b, *
GLK1	0.566	0	1	Glucokinase, specific for aldohexoses	a
KRS1	0.537	0.469	2	Lysyl-tRNA synthetase, cytoplasmic	
OSH2	0.52	0.232	2	Member of an oxysterol-binding protein family involved in sterol metabolism	
SEC13	0.52	0	1	Component of the COPII coat of vesicles involved in ER to Golgi transport	
ADH1	0.519	0.171	3	Alcohol dehydrogenase I, cytoplasmic isozyme reducing acetaldehyde to ethanol, regenerating NAD+	
RPL22A	0.511	0	1	Ribosomal protein L22	
SPT6	0.5	0.247	2	Protein involved in chromatin structure that influences expression of many genes	
GUS1	0.488	0.079	2	Glutamyl-tRNA synthetase, member of the class I aminoacyl tRNA synthetase family	a
CDC46	0.477	0	1	Member of the MCM/P1 family, component of the MCM complex that binds at ARS elements to initiate DNA replication	b
PRX1	0.458	0	1	Mitochondrial thiol peroxidase	
NRD1	0.41	0	1	Protein that controls transcriptional elongation and poly(A)-independent 3' end formation,	

Gene	204/WT	SD	Peptides	Gene Product	Ub
SEC8	0.407	0	1	Component of the exocyst complex that is required for exocytosis, required for normal ER and Golgi inheritance	
ARC1	0.397	0.181	4	Cofactor for methionyl- and glutamyl-tRNA synthetases and G4 quadruplex nucleic acid binding protein	
SNX4	0.384	0	1	Putative nexin sorting protein, involved in retrograde transport, possibly involved in proteasome function	
HSP78	0.367	0.36	6	Mitochondrial heat shock protein of the ClpB family of ATP-dependent proteases	
IDH1	0.322	0.222	12	Isocitrate dehydrogenase (NAD+) subunit 1, mitochondrial, required for oxidative function of the tricarboxylic acid cycle	
YKL056C	0.322	0.071	3	Protein possibly involved in cytoplasmic ribosome function, has similarity to translationally controlled tumor protein (TCTP)	
MEX67	0.321	0	1	Protein involved in the export of mRNA from the nucleus to the cytoplasm	
SER33	0.309	0	1	3-phosphoglycerate dehydrogenase, catalyzes the first step in the synthesis of serine from 3-phosphoglycerate	
RPS13	0.305	0.14	3	Ribosomal protein S13	
FBA1	0.294	0.223	6	Fructose-bisphosphate aldolase II, involved in glycolysis	
RPN9	0.282	0.273	26	Non-ATPase subunit of the 26S proteasome complex, required for efficient assembly of the complex, also functions in RNA polymerase II transcription elongation	
LSC1	0.275	0.083	3	Alpha subunit of succinyl-CoA synthetase (succinyl-CoA ligase, succinate thiokinase)	a
RPL21B	0.265	0	1	Ribosomal protein L21	b, c
PRT1	0.261	0.017	2	Translation initiation factor eIF3 beta subunit (p90), has an RNA recognition (RRM) domain	
ARO4	0.246	0.013	2	2-Dehydro-3-deoxyphosphoheptonate aldolase (DAHP synthase), inhibited by tyrosine	
RPL13A	0.24	0	1	Ribosomal protein L13	d
STE20	0.237	0.02	3	Serine/threonine protein kinase of the pheromone response pathway	
HSP82	0.236	0.156	13	Heat-inducible chaperonin homologous to E. coli HtpG and mammalian HSP90, involved in control of lysine biosynthesis	b
TRP2	0.215	0	1	Component I of anthranilate synthase:indole-3-glycerol phosphate synthase (anthranilate synthase), involved in tryptophan biosynthesis pathway	
IDH2	0.211	0.139	8	Isocitrate dehydrogenase (NAD+) subunit 2, mitochondrial, required for oxidative function of the tricarboxylic acid cycle	

Gene	204/WT	SD	Peptides	Gene Product	Ub
RPN12	0.21	0.148	26	Non-ATPase component of 26S proteasome complex, required for activation of Cdc28p protein kinase and functions in RNA polymerase II transcription elongation	
RPS23A	0.203	0.046	2	Ribosomal protein S23	
RPL25	0.201	0.167	3	Ribosomal protein L25	
IWS1	0.188	0	1	Protein involved in transcription regulation	
RPS7B	0.173	0.152	2	Ribosomal protein S4	
ACS2	0.17	0	1	Acetyl-CoA synthetase (acetate-CoA ligase)	c
YHR020W	0.167	0	1	Putative prolyl-tRNA synthetase, member of the class II family of aminoacyl-tRNA synthetases	
RPS16B	0.157	0	1	Ribosomal protein S16	
RPL3	0.145	0.121	4	Ribosomal protein L3	b, c
NAP1	0.144	0.095	6	Nucleosome assembly protein that plays a role in assembly of histones into octamer, required for full expression of Clb2p functions	
SEC31	0.129	0.022	2	Component (p150) of the COPII coat of secretory pathway vesicles involved in ER to Golgi transport	
GGA2	0.121	0.111	5	Protein involved in trafficking of proteins between the trans-Golgi network and the vacuole	a, b
VAS1	0.12	0	1	Valyl-tRNA synthetase	
ARG1	0.118	0	1	Argininosuccinate synthetase, catalyzes the penultimate step in arginine synthesis	
MLC1	0.118	0	1	Myosin light chain required for cytokinesis	
RPS8A	0.114	0.107	3	Ribosomal protein S8	
SLY1	0.106	0	1	Protein involved in vesicle trafficking between ER and Golgi, member of the Sec1p family, component of the early Golgi SNARE complex	
GND1	0.103	0.059	2	6-Phosphogluconate dehydrogenase, decarboxylating, converts 6-phosphogluconate + NADP to ribulose-5-phosphate + NADPH + CO2	
SEM1	0.085	0	1	Structural component of the 26S proteasome lid, regulates exocytosis and pseudohyphal differentiation in yeast	
RFC2	0.077	0	1	Replication factor C, second subunit, homologous to human 37 kDa subunit, may play a role in establishing sister chromatid cohesion	
SAH1	0.057	0	1	Adenosylhomocysteinase (S-adenosylhomocysteine hydrolase)	
SSE1	0.036	0.027	2	Heat shock protein of the HSP70 family, retains heat-denatured proteins in a folding-competent conformation, multicopy suppressor of mutants with hyperactivated ras/cAMP pathway	
RPL5	0.027	0	1	Ribosomal protein L5, the sole 5S rRNA-associated ribosomal protein	d
RNA1	0.023	0	1	GTPase-activating (GAP) protein for Gsp1p (Ran), involved in nuclear export	
ADE5,7	0.007	0	1	Phosphoribosylamine-glycine ligase (GARSase) plus phosphoribosylformylglycinamidine cyclo-ligase (AIRSase)	
ENT3	0.006	0	1	Epsin homolog required for endocytosis	

Figure 4-5. List of proteins enriched in *uba1-204* proteasomes. Genes identified as enriched in *uba1-204* affinity purified 26S proteasome sample

compared to wild-type sample. "204/WT" reflects the ratio of $^{14}N/^{15}N$ isotope-labeled peptides, "SD" lists the standard deviation, and "peptides" is the number of peptides identified for each protein. The column entitled "Ub" denotes proteins which have been identified in the following published mass spectrometry experiments: a) Peng et al. 2003; b) Hitchcock et al. 2003; c) Mayor et al. 2005; d) Verma et al. 2004. Asterisk denotes proteins shown to be ubiquitinated in other studies. The ubiquitination of Taf5 is described in Auty et al. (2004) and ubiquitination of Rvs167 is described in Stamenova et al. (2004).

In an attempt to validate the result showing increased levels of Cic1 at *uba1-204* proteasomes, we obtained Cic1 antibody from the laboratory of Dr. Dieter Wolf. Unfortunately, our results were inconclusive using the crude anti-Cic1 serum provided. However, considering this protein's role as an adaptor protein, recruiting Cdc4 and Grr1 for degradation by the proteasome (Jager et al. 2001), our study highlights the importance of further analysis of the possible regulation of the interaction of this protein with the proteasome.

DISCUSSION

In this study, we describe the first application of MudPIT to the examination of proteasome complexes isolated in the absence of ubiquitin chains. Although experimental validation of the findings described here is beyond the scope of this study, we have provided a useful survey of the spectrum of proteins that are targeted to the proteasome.

These data confirmed that intact proteasome complexes can be purified from *uba1-204* cells and that all subunits of the proteasome are present with little variation on their abundance. Furthermore, it is possible to gain some valuable insights into the future potential of proteomic analysis of *uba1-204* cells by comparing our results to previously published works.

We had anticipated identifying potential novel substrates of the ubiquitin-proteasome pathway in the proteins that were depleted in the mutant sample. Indeed, one of the most depleted proteins, the Sec23 component of COPII coat of vesicles, was identified by three peptides and is known to be polyubiquitinated and degraded by the proteasome (Cohen et al. 2003). Intriguingly, we also encountered all proteins involved in the formation of the coat protein complex (COPII), which produces transport vesicles to mediate export of proteins from the endoplasmic reticulum. Transport vesicle formation begins when the GTPase Sar1 associates with the ER membrane and recruits a protein complex, which includes Sec23, Sec24, Sec13, and Sec31. Sec23 is regulated by ubiquitination, which disrupts its interaction with Sec24 because of a direct effect of ubiquitination on protein conformation or association of the monoubiquitinated Sec23 with ubiquitination machinery, such as the proteasome (Cohen et al. 2003). Cohen et al. have shown that Ubp3-Bre5 complex is required to cleave the first conjugated ubiquitin from Sec23, resulting in accumulation of monoubiquitinated Sec23. This facilitates subsequent polyubiquitination and degradation by the proteasome. Thus, the balance between polyubiquitination of Sec23 and its deubiquitination and rescue from degradation by Ubp3-Bre5 controls Sec23 levels in order to regulate cell growth and viability (Cohen et al. 2003).

The decrease in Sec23 protein observed at *uba1-204* proteasomes further establishes its role as a ubiquitin pathway substrate and provides a validation of the

strategy described here to identify substrates by analyzing peptides depleted in proteasome complexes isolated in *uba1-204* cells. In addition, our identification of the entire COPII complex lends support to the hypothesis described in Cohen et al. that the proteasome may associate directly with ubiquitinated Sec23 at the site of the COPII vesicle formation. Interestingly, all three proteins that combine with Sec23 to form the COPII vesicle, Sec13, Sec31, and Sec24, are enriched at proteasomes in the absence of polyubiquitin.

While we had expected to observe ubiquitinated proteasome substrate proteins depleted in *uba-204* cells, it was less clear what types of proteins would be enriched in the mutant proteasomes. We reasoned that with very few normal substrates being targeted to the proteasome, it would be possible to identify a unique set of proteasome-interacting proteins. This may include adaptor proteins, ubiquitin-independent substrates, proteins with lower affinity for the proteasome, or monoubiquitinated proteins. By focusing on a few proteins identified in the results, it is possible to gain an idea of the proteomic environment in proteasomes in *uba1-204*.

Cic1 was isolated in our screen as the protein most enriched in proteasomes isolated in the absence of Uba1 activity. Cic1 interacts *in vitro* and *in vivo* with the proteasome and with Cdc4 and thought to act as an adaptor protein, recruiting F-box proteins Cdc4 and Grr1 for degradation (Jager et al. 2001). *Cic1* mutants stabilize Cdc4 and Grr1, substrate recognition subunits of the SCF complex (Jager et al. 2001). If this protein indeed functions as an adaptor mediating the degradation of specific, important ubiquitin-proteasome pathway substrates, its increased presence in proteasomes isolated from *uba1-204* cells suggests that its docking onto the proteasome is regulated.

Mex67 is an mRNA nuclear export receptor that contains a UBA domain that is required for proper mRNA export (Gwizdek et al. 2006). Mex67 interacts with ubiquitin chains and with Hpr1, a protein that couples transcription to mRNA export. The interaction with Mex67 is required to protect Hpr1 from ubiquitination and degradation (Gwizdek et al. 2006). Rvs167, a protein involved in receptor internalization and organization of the actin cytoskeleton, was shown to be ubiquitinated in earlier mass spectrometry studies (Peng et al. 2003; Hitchcock et al. 2003) and found to be enriched in this study. Recently, it was verified that monoubiquitination of Rvs167 by the Rsp5 ligase regulates a protein complex required for endocytosis (Stamenova et al. 2004).

In summary, our findings provide additional support to earlier mass spectrometric studies that sought to identify new candidate substrates of the ubiquitin-proteasome system. Furthermore, we have found examples of the merit of using *uba1-204* in analyzing ubiquitin's many other activities beyond proteolysis, such as vesicle trafficking, mRNA export, and endocytosis. While the large amount of information provided in this study provides more questions than answers, it highlights the value of this novel genetic mutant in uncovering new cellular roles for ubiquitin. By enabling broad shutdown of all cellular ubiquitination in a matter of minutes, we can delve into the countless cellular processes that require this truly ubiquitous protein.

MATERIALS AND METHODS

Preparation of extracts for affinity purification of 26S proteasomes

Yeast strains were grown to log phase at 25°C in medium containing 0.67% yeast nitrogen base minus amino acids, 2% dextrose, 0.5% ammonium sulfate. Cultures were diluted to OD_{600} = 0.008, with wild-type culture media containing ^{15}N ammonium sulfate and *uba1-204* media containing ^{14}N ammonium sulfate. This allows wild-type cells to grow for at least 7 generations in order to label all proteins with the "heavy" nitrogen. At OD_{600} = 1, cultures were filtered and resuspended in media which was prewarmed to 37°C. Cultures were incubated at 37°C for 20 minutes and pelleted by centrifugation for 5 minutes at 37°C. Pellets were washed with sterile water and flash frozen in liquid nitrogen.

Frozen cell pellets were ground to a fine powder under liquid nitrogen in a mortar placed on a bed of dry ice. Powder was resuspended in one pellet-volume of column buffer containing 50 mM Tris, pH 7.5, 150 mM NaCl, 10% glycerol, 5 mM $MgCl_2$, 5 mM ATP. ATP Regenerating System (ARS) (Verma et al. 1997) was added and the lysates were clarified by centrifugation at 17,000 rpm for 20 minutes.

Lysates were supplemented again with 5 mM ATP and 5 mM $MgCl_2$ and incubated at 4°C for 2 hours with FLAG antibody-coupled beads from Sigma (St. Louis, MO) that had been prewashed in 0.1 M glycine, pH3.5 and resuspended as a 50% slurry with column buffer. For each sample, 1.5 ml of lysate was incubated with 1 ml bead slurry. Bead-bound proteins were pelleted and washed three times with high salt wash buffer consisting of the column buffer described above supplemented with 0.2% Triton X-100 and NaCl to a final concentration of 200 mM. Bead-bound proteins were then washed twice with low-salt

wash buffer containing 50 mM Tris-HCl, pH7.5, 20 mM $MgCl_2$, 2 mM ATP. All supernatant was aspirated with a 25 gauge needle and the pellet was resuspended in three times its volume of elution buffer containing 25 mM Tris, pH7.5, 150 mM NaCl, 5 mM $MgCl_2$, 2 mM ATP, and 100 μg/ml Flag peptide and proteins were eluted at 4°C for 3 hours.

Mass Spectrometry and Data Analysis

To generate peptides for mass spectrometry, proteasome samples were incubated with 3 mM Tris-(2-carboxyethyl)phosphine (T-CEP) for 20 minutes and then for another 15 minutes following addition of iodoacetamide to 11 mM. 0.3 g Endoproteinase Lys-C (Boehringer Mannheim) was added and the sample was then digested for 6 hours at 37°C. Samples were diluted with buffer (100 mM Tris-HCl, pH 8.0, 1.33 mM $CaCl_2$) and incubated with 1 μg of trypsin (Roche Applied Science) overnight at 37°C.

Samples were processed for multidimensional chromatography as described in Graumann et al. (2004). MS/MS spectra recorded by Xcaliber (ThermoElectron) were analyzed for charge state and controlled for data quality by 2to3 (Sadygov et al. 2002). Results were searched against translated open reading frames of the *Saccharomyces* Genome Database (SGD) (Cherry et al. 1998). The spectra generated were evaluated using algorithms from Sequest (Eng et al. 1994) and DTASelect/Contrast (Tabb et al. 2002) and quantification software RelEx (MacCoss et al. 2003) was used to generate comparative results.

Chapter 5

FINDINGS AND IMPLICATIONS

One of the major contributions of this thesis is the creation and characterization of the first strong loss-of-function conditional allele of *Saccharomyces cerevisiae UBA1* gene. *Uba1-204* provides a new method for genetically inhibiting the ubiquitin-proteasome pathway in yeast. The most striking result was the loss of all detectable ubiquitin conjugates within five minutes of incubation at the nonpermissive temperature. This suggests an unprecedented mechanism for shutdown of ubiquitin-dependent cellular functions. Furthermore, this conditional phenotype is reversible with similarly fast kinetics. This renders it necessary to maintain mutant cells at the nonpermissive temperature; however, it simultaneously increases the usefulness of this mutant in future experiments. In characterizing this allele, we have demonstrated strong stabilization of a range of substrate proteins. However, considering that at least one protein, Clb2, has been shown to be unaffected, it remains to be seen how broad these protein stabilization effects are. Certainly this mutant strain will prove valuable in determining the ubiquitin dependence or ubiquitin independence of pathway substrates and could help to identify new substrates or even new ubiquitin-dependent processes. It may also provide hints to better understanding the structure-function relationships of E1 and E1-like proteins.

Furthermore, we have employed the cellular loss of ubiquitin chains to address an unanswered question regarding the proteasomal targeting of ubiquitinated substrates. Rad23 is known to recognize ubiquitin chains via its UBA domain and to bind to the proteasome via its UbL domain. However, it was previously unknown which process

occurred first. By investigating the affect of ubiquitin-chain depletion on Rad23 targeting function, we were able to provide clues to the mechanistic details involved in this process. Our results reveal that Rad23 engages with ubiquitin chains prior to its association with the proteasome, providing evidence to support the "shuttle factor" model of substrate targeting. It would have been difficult to distinguish between the two proposed models without a method of inhibiting ubiquitination. Another aspect of our findings was that in addition to ubiquitinated substrate, free ubiquitin chains are also sufficient to trigger Rad23 shuttling. If free ubiquitin chains can exploit Rad23 binding activity *in vivo*, our data suggest that they could compete with ubiquitinated substrates for proteasome targeting as well.

The finding that ubiquitin chains are required for efficient targeting of ubiquitin-binding receptors to the proteasome further demonstrated that proteasome complexes isolated from *uba1-204* cells contained a unique "interactome" of proteins. To explore the global effects of this ubiquitin pathway block, we examined the proteomic profile of proteins that copurified with proteasome complexes in the presence and absence of Uba1 activity using MudPIT. This initial proteomic analysis of proteasomes isolated from mutant cells hints at the potential of this method in identifying novel substrates, adaptors, and regulators of the proteasome.

Overall, this thesis provides characterization of a valuable new genetic tool for inhibiting the ubiquitin-proteasome pathway. This research makes a significant contribution towards elucidating the molecular mechanisms involved in regulating the targeting of ubiquitinated proteins to the proteasome. It is my hope that this work will contribute to further exploration of the many roles that ubiquitin plays in proteolysis, as well as in other ubiquitin-dependent cellular processes.

APPENDIX I: STRAIN LIST AND PLASMID MAP

STRAIN LIST

Note: Mat a strains are sterile due to a partial deletion of the overlapping *STE6* gene.

Strain	Genotype	Reference
RJD381	*diploid, can1-100, leu2-3, -112, his3-11, -15, trp1-1, ura3-1, ade2-1*	Laboratory collection
RJD3267	RJD381, *ubaΔ::KanMX*	This study
RJD3491	*Mat alpha, uba1Δ::KanMX, [pRS313-UBA1::HIS], can1-100, leu2-3, -112, his3-11, -15, trp1-1, ura3-1, ade2-1*	This study
RJD3290	*Mat alpha, uba1Δ::KanMX, [pRS313-uba1-204::HIS], can1-100, leu2-3, -112, his3-11, -15, trp1-1, ura3-1, ade2-1*	This study
RJD3268	*Mata, uba1Δ::KanMX, [pRS313-UBA1::HIS], can1-100, leu2-3, -112, his3-11, -15, trp1-1, ura3-1, ade2-1*	This study
RJD3269	*Mata, uba1Δ::KanMX, [pRS313-uba1-204::HIS], can1-100, leu2-3, -112, his3-11, -15, trp1-1, ura3-1, ade2-1*	This study
RJD3270	RJD3268, *ura3::PGAL-SIC1HA*	This study
RJD3271	RJD3268, *[PGAL-UbV76-V-βgal::URA3]*	This study
RJD3272	RJD3268, *ura3-52::PTDH3-Deg1-GFP::URA*	This study
RJD3273	RJD3269, *ura3::PGAL-SIC1HA*	This study
RJD3274	RJD3269, *[PGAL-UbV76-V-βgal::URA3]*	This study
RJD3275	RJD3269, *ura3-52::PTDH3-Deg1-GFP::URA*	This study
RJD3276	RJD3491, *ADE2, LEU2, TRP1, PRE1FH::YIplac211::URA*	This study
RJD3277	RJD3490, *ADE2, LEU2, TRP1, PRE1FH::YIplac211::URA*	This study
RJD3983	RJD3491, *pdr5Δ::HIS, ADE2, LEU2, TRP1, PRE1FH::YIplac211::URA*	This study
RJD3984	RJD3490, *pdr5Δ::HIS, ADE2, LEU2, TRP1, PRE1FH::YIplac211::URA*	This study
Plasmids		
RDB1837	*[pRS313-UBA1::HIS]*	This study
RDB1838	*[pRS313-uba1-60::HIS]*	This study
RDB1839	*[pRS313-uba1-108::HIS]*	This study
RDB1840	*[pRS313-uba1-126::HIS]*	This study
RDB1841	*[pRS313-uba1-204::HIS]*	This study

PLASMID MAP OF PRS313-UBA1

Map of pRS313-UBA1. The UBA1 gene was cloned into the linker region of the *Saccharomyces/E. coli* CEN vector pRS313 to generate RDB1837. The gene includes the endogenous promoter and terminator regions to drive expression, including 186 base pairs upstream of the start codon and 269 base pairs downstream of the stop codon.

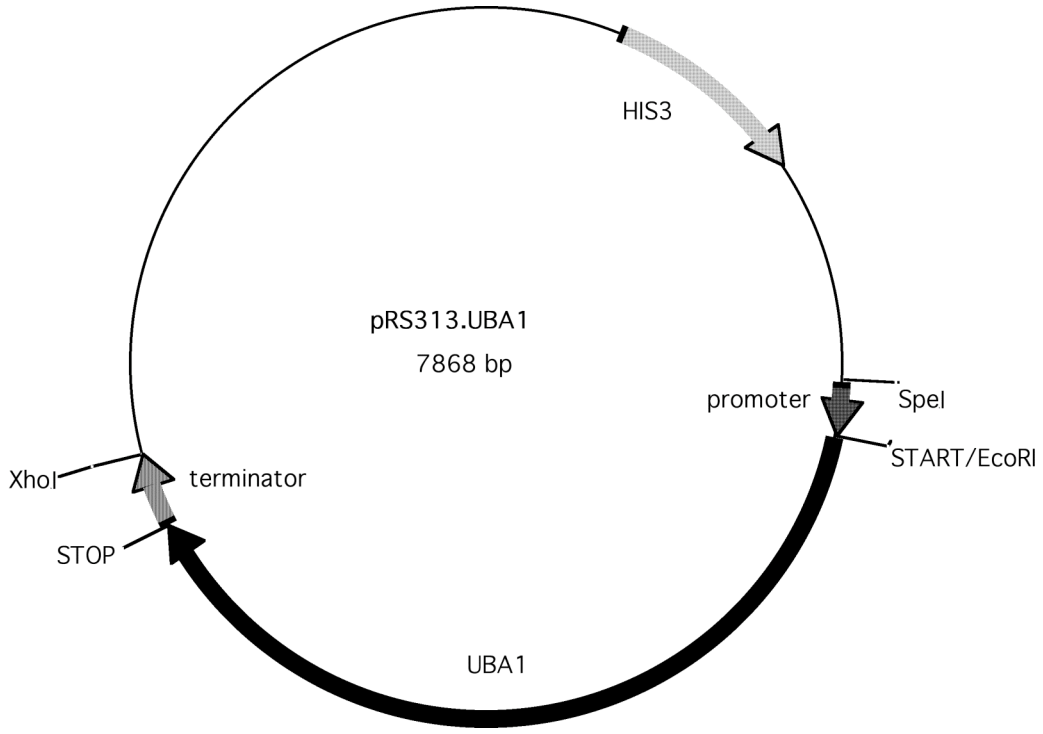

REFERENCES

Amerik, A. Y. and Hochstrasser, M. (2004). Mechanism and function of deubiquitinating enzymes. *Biochem Biophys Acta,* **1695**, 189-207.

Auty, R., Steen, H., Myers, L. C., Persinger, J., Bartholomew, B., Gygi, S. P., and Buratowski, S. (2004). Purification of active TFIID from *Saccharomyces cerevisiae*. *J Biol Chem,* **279**, 49973-49981.

Babbitt, S. E., Kiss, A., Deffenbaugh, A. E., Chang, Y. H., Bailly, E., Erdjument-Bromage, H., Tempst, P., Buranda, T., Sklar, L. A., Baumler, J., Gogol, E., and Skowyra, D. (2005). ATP hydrolysis-dependent disassembly of the 26S proteasome is part of the catalytic cycle. *Cell,* **121**, 553-565.

Bertolaet, B. L., Clarke, D. J., Wolff, M., Watson, M. H., Henze, M., Divita, G., and Reed, S. I. (2001a). UBA domains mediate protein-protein interactions between two DNA damage-inducible proteins. *J Mol Biol,* **313**, 995-963.

Bertolaet, B. L., Clarke, D. J., Wolff, M., Watson, M. H., Henze, M., Divita, G., and Reed, S. I. (2001b). UBA domains of DNA damage-inducible proteins interact with ubiquitin. *Nat Struct Mol Biol,* **8**, 47-422.

Biggins, S., Ivanovska, I., and Rose, R. D. (1996). Yeast ubiquitin-like genes are involved in duplication of the microtubule organizing center. *J Cell Biol,* **133**, 1331-1346.

Chen, L., and Madura, K. (2002). Rad23 promotes the targeting of proteolytic substrates to the proteasome. *Mol Cell Biol,* **22**, 4902-4913.

Cheng, I. H., Roberts, L. A., and Tye, B. K. (2002). Mcm3 is polyubiquitinated during mitosis before establishment of the pre-replication complex. *J Biol Chem,* **277**, 41706-41714.

Cherry, J. M., Adler, C., Ball, C., Chervitz, S. A., Dwight, S. S., Hester, E. T., Jia, Y., Juvik, G., Roe, T., Schroeder, M., Weng, S., and Botstein, D. (1998). SGD: *Saccharomyces* Genome Database. *Nucleic Acids Res,* **26**, 73-79.

Ciechanover, A. (1998). The ubiquitin-proteasome pathway: On protein death and cell life. *EMBO J*, **17**, 7151-7160.

Ciechanover, A. (2005). Proteolysis: From the lysosome to ubiquitin and the proteasome. *Nat Rev Mol Cell Biol,* **6**, 79-86.

Ciechanover, A., Finley, D., and Varshavsky, A. (1984). Ubiquitin dependence of selective protein degradation demonstrated in the mammalian cell-cycle mutant ts85. *Cell,* **37***,* 57-66.

Ciechanover, A., Heller, H., Katz-Etzion, R., and Hershko, A. (1981). Activation of the heat-

stable polypeptide of the ATP-dependent proteolytic system. *Proc Natl Acad Sci USA,* **78**, 761-765.

Cohen, M., Stutz, F., Belgareh, N., Haguenauer-Tsapis, R., and Dargemont, C. (2003). Ubp3 requires a cofactor, Bre5, to specifically de-ubiquitinate the COPII protein, Sec23. *Nat Cell Biol,* **5**, 661-667.

Cohen, M., Stutz, F., and Dargemont, C. (2003). Deubiquitination, a new player in Golgi to endoplasmic reticulum retrograde transport. *J Biol Chem,* **278**, 51989-51992.

Daugherty, P. S., Chen, G., Iverson, B. L., and Georgiou, G. (2000). Quantitative analysis of the effect of the mutation frequency on affinity maturation of single chain Fv antibodies. *Proc Natl Acad Sci USA,* **97**, 2029-2034.

Deshaies, R. J. (1999). SCF and Cullin/Ring H2-based ubiquitin ligases. *Annu Rev Cell Dev Biol,* **15**, 435-467.

Deshaies, R. J., Seol, J. H., McDonald, W. H., Cope, G., Lyapina, S., Shevchenko, A., Shevchenko, A., Verma, R., and Yates III, J. R. (2002). Charting the protein complexome in yeast by mass spectrometry. *Molecular and Cellular Proteomics,* **1**, 3-10.

Deveraux, Q., Ustrell, V., Pickart, C. M., and Rechsteiner, M. (1994). A 26S protease subunit that binds ubiquitin conjugates. *J Biol Chem,* **269**, 7059-7061.

Elsasser, S., Chandler-Militello, D., Muller, B., Hanna, J., and Finley, D. (2004). Rad23 and Rpn10 serve as alternative ubiquitin receptors for the proteasome. *J Biol Chem,* **279**, 26817-26822.

Elsasser, S., and Finley, D. (2005). Delivery of ubiquitinated substrates to protein-unfolding machines. *Nat Cell Biol,* **7**, 742-749.

Elsasser, S., Gali, R. R., Schwickart, M., Larsen, C. N., Leggett, D. S., Muller, B., Feng, M. T., Tubing, F., Dittmar, G. A., and Finley, D. (2002). Proteasome subunit Rpn1 binds ubiquitin-like protein domains. *Nat Cell Biol,* **4**, 725-730.

Eng, J. K., McCormack, A. L., and Yates III, J. R. (1994). An approach to correlate tandem mass-spectral data of peptides with amino-acid sequences in a protein database. *J Am Soc Mass Spectr,* **5**, 976-989.

Finley, D., Ciechanover, A., and Varshavsky, A. (1984). Thermolability of ubiquitin-activating enzyme from the mammalian cell-cycle mutant ts85. *Cell,* **37**, 43-55.

Finley, D., Ciechanover, A., and Varshavsky, A. (2004). Ubiquitin as a central regulator. *Cell*, **116**, 29-32.

Funakoshi, M., Sasaki, T., Nishimoto, T., and Kobayashi, H. (2002). Budding yeast Dsk2p is a polyubiquitin-binding protein that can interact with the proteasome. *Proc Natl Acad Sci USA,* **99**, 745-750.

Gandre, S., and Kahana, C. (2002). Degradation of ornithine decarboxylase in *Saccharomyces cerevisiae* is ubiquitin independent. *Biochem Biophys Res Commun*, **293**, 139-144.

Ghaboosi, N., and Deshaies, R. J. (2007). A conditional yeast E1 mutant blocks the ubiquitin-proteasome pathway and reveals a role for ubiquitin conjugates in targeting Rad23 to the proteasome. *Mol Biol Cell,* **18**, 1953-1963.

Glickman, M. H., Rubin, D. M., Fried, V. A., and Finley, D. (1998). The regulatory particle of the *Saccharomyces cerevisiae* proteasome*. Mol Cell Biol* **18,** 3149-3162.

Goebl, M. G., Yochem, J., Jentsch, S., McGrath, J. P., and Finley, D. (1998). The yeast cell-cycle gene CDC34 encodes a ubiquitin-conjugating enzyme. *Science,* **241**, 1331-1335.

Golddstein, G., Steed, M., Hammerling, U., Boyse, E. A., Schlesinger, D. H., and Niall, H. D. (1975). Isolation of a polypeptide that has lymphocyte-differentiating properties and is probably represented universally in living cells. *Proc Natl Acad Sci USA,* **72**, 11-15.

Goldknopf, I. L., and Busch, H. (1977). Isopeptide linkage between nonhistone and histone 2A polypeptides of chromosomal conjugate protein A2A. *Proc Natl Acad Sci USA,* **74**, 864-868.

Graumann, J. (2006). Implementation of Multidimensional Protein Identification Technology and its application to the characterization of protein complexes in bakers yeast. *Ph.D. Dissertation*, Pasadena, CA: California Institute of Technology Press.

Graumann, J., Dunipace, L. A., Seol, J. H., McDonald, W. H., Yates III, J. R., Wold, B. J., and Deshaies, R. J. (2004). Applicability of tandem affinity purification MudPIT to pathway proteomics in yeast. *Molecular and Cellular Proteomics*, **3**, 226-237.

Guthrie, C., and Fink, G. R. (1991). *Methods in Enzymology*, Volume 194: Guide to Yeast Genetics and Molecular Biology. New York: Academic Press.

Gwizdek, C., Iglesias, N., Rodriguez, M. S., Ossareh-Nazari, B., Hobeika, M., Divita, G., Stutz, F., and Dargemont, C. (2006). Ubiquitin-associated domain of Mex67 synchronizes recruitment of the mRNA export machinery with transcription. *Proc Natl Acad Sci USA,* **103**, 16376-16381.

Haas, A. L., Bright, P. M., and Jackson, V. E. (1988). Functional diversity among putative E2 isozymes in the mechanism of ubiquitin-histone ligation. *J Biol Chem*, **263**, 13268-13275.

Haas, A. L., and Siepmann, T. J. (1997). Pathways of ubiquitin conjugation. *FASEB J*, **11**, 1257-1268.

Haracska, L., and Udvardy, A. (1995). Cloning and sequencing a non-ATPase subunit of the regulatory complex of the Drosophila 26S protease. *Eur J Biochem*, **231**, 720-725.

Hershko, A., Ciechanover, A., Heller, H., Haas, A. L., and Rose, I. A. (1980). Proposed role of ATP in protein breakdown: Conjugation of proteins with multiple chains of the polypeptide of ATP-dependent proteolysis. *Proc Natl Acad Sci USA,* **77**, 1783-1786.

Hershko, A., Ciechanover, A., and Varshavsky, A. (2000). The ubiquitin system. *Nat Med* **6**,

1073-1081.

Hershko, A., Heller, H., Elias, S., and Ciechanover, A. (1983). Components of the ubiquitin-proteasome ligase system: Resolution, affinity purification and role in protein breakdown. *J Biol Chem,* **258**, 8206-8214.

Hicke, L., Schubert, H. L., and Hill, C. P. (2005). Ubiquitin-binding domains. *Nat Rev Mol Cell Biol*, **6**, 610-621.

Hitchcock, A. L., Auld, K., Gygi, S. P., and Silver, P. A. (2003). A subset of membrane-associated proteins is ubiquitinated in response to mutations in the endoplasmic reticulum degradation machinery. *Proc Natl Acad Sci USA,* **100**, 12735-12740.

Hochstrasser, M. (1998). There's the Rub: a novel ubiquitin-like modification linked to cell-cycle regulation. *Genes Dev,* **12**, 901-907.

Hofmann, K., and Bucher, P. (1996). The UBA domain: a sequence motif present in multiple enzyme classes of the ubiquitin pathway. *Trends in Biochemical Science***, 21**, 172-173.

Jager, S., Strayle, J., Heinemeyer, W., and Wolf, D. H. (2001). Cic1, an adaptor protein specifically linking the 26S proteasome to its substrate, the SCF component Cdc4. *EMBO J,* **20**, 4423-4431.

Johnson, E. S., Ma, P. C. M., and Ota, I. M. (1995). A proteolytic pathway that recognizes ubiquitin as a degradation signal. *J Biol Chem,* **270**, 17442-17456.

Kamionka, M., and Feigon, J. (2004). Structure of the XPC binding domain of hHR23A reveals hydrophobic patches for protein interaction. *Prot Sci,* **13**, 2370-2377.

Kang, Y., Vossler, R. A., Diaz-Martinez, L. A., Winter, N. S., Clarke, D. J., and Walters, K. J. (2006). UBL/UBA ubiquitin receptor proteins bind a common tetraubiquitin chain. *J Mol Biol,* **356,** 1027-1035.

Kim, I., Mi, K., and Rao, H. (2004). Multiple interactions of Rad23 suggest a mechanism for ubiquitylated substrate delivery important in proteolysis. *Mol Biol Cell*, **15**, 3357-3365.

Kleijnen, M. F., Shih, A. H., Zhou, P., Kumar, S., Soccio, R. E., Kedersha, N. L., Gill, G., and Howley, P. M. (2000). The hPLIC proteins may provide a link between the ubiquitination machinery and the proteasome. *Mol Cell,* **6**, 409-419.

Kulka, R. G., Raboy, B., Schuster, R., Parag, H. A., Diamond, G., Ciechanover, A., and Marcus, M. (1988). A Chinese hamster cell-cycle mutant arrested at G2 phase has a temperature-sensitive ubiquitin-activating enzyme, E1. *J Biol Chem,* **263**, 15726-15731.

Lake, M. W., Wuebbens, M. M., Rajagopalan, K. V., and Schindelin, H. (2001). Mechanism of ubiquitin activation revealed by the structure of a bacterial MoeB-MoaD complex. *Nature*, **414**, 325-329.

Lambertson, D., Chen, L., and Madura, K. (1999). Pleiotropic defects caused by loss of the

proteasome-interacting factors Rad23 and Rpn10 of *Saccharomyces cerevisiae*. *Genetics*, **153**, 69-79.

Link, A. J., Eng, J. K., Schieltz, D. M., Carmack, E., Mize, G. J., Morris, D. R., Garvik, B. M., Yates III, J. R. (1999). Direct analysis of protein complexes using mass spectrometry. *Nat Biotechnol,* **17**, 676-682.

Lowe, E. D., Hasan, N., Trempe, J. F., Fonso, L., Noble, M. E. M., Endicott, J.A., Johnson, L.N., and Brown, N.R. (2006). Structures of the Dsk2 UBL and UBA domains and their complex. *Acta Crystallogr D Biol Crystallogr*, **62,** 177-188.

MacCoss, M. J., Wu, C. C., Liu, H., Sadygov, R., and Yates III, J. R. (2003).A correlation algorithm for the automated quantitative analysis of shotgun proteomics data. *Anal Chem*, **75**, 6912-6921.

Madura, K. (2004). Rad23 and Rpn10: Perennial wallflowers join the melee. *Trends Biochem Sci*, **29**, 637-640.

Mayor, T., Lipford, J. R., Graumann, J., Smith, G. T., and Deshaies, R. J. (2005). Analysis of polyubiquitin conjugates reveals that the Rpn10 substrate receptor contributes to the turnover of multiple proteasome targets. *Mol Cell Proteomics*, **4**, 741-751.

McGrath, J.P. (1991). Molecular genetic analysis of the ubiquitin-protein ligase system of Saccharomyces cerevisiae. *Ph.D. Dissertation*, Cambridge, MA: Massachusetts Institute of Technology Press.

McGrath, J.P., Jentsch, S., and Varshavsky, A. (1991). UBA1: an essential yeast gene encoding ubiquitin-activating enzyme. *EMBO J*, **10**, 227-236.

Oda, Y., Huang, K., Cross, F.R., Cowburn, D., and Chait, B.T. (1999). Accurate quantitation of protein expression and site-specific phosphorylation. *Proc Natl Acad Sci USA,* **96**, 6591-6596.

Ortolan, T.G., Tongaonkar, P., Lambertson, D., Chen, L., Schauber, C., and Madura, K. (2000). The DNA repair protein Rad23 is a negative regulator of multiubiquitin chain assembly. *Nat Cell Biol*, **2**, 601-608.

Palanimurugan, R., Scheel, H., Hofmann, K., and Dohmen, J. (2004). Polyamines regulate their synthesis by inducing expression and blocking degradation of ODC antizyme. *EMBO J*, **23**, 4857-4867.

Peng, J., Schwartz, D., Elias, J. E., Thoreen, C. C., Cheng, D., Marsischky, G., Roelofs, J., Finley, D., and Gygi, S. P. (2003). A proteomics approach to understanding protein ubiquitination. *Nat Biotechnol***, 21**, 921-926.

Pickart, C. M., and Cohen, R. E. (2004). Proteasomes and their kin: proteasomes in the machine age. *Nat Rev Mol Cell Biol*, **5**, 177-187.

Pickart, C. M., and Rose, I. A. (1985). Ubiquitin carboxyl-terminal hydrolase acts on ubiquitin carboxyl-terminal amides. *J Biol Chem,* **260**, 7903-7910.

Raasi, S., Orlov, I., Fleming, K. G., and Pickart, C. M. (2004). Binding of polyubiquitin chains to ubiquitin-associated (UBA) domains of hHR23A. *J Mol Biol,* **341**, 1367-1379.

Raasi, S., and Pickart, C. M. (2003). Rad23 ubiquitin-associated domains (UBA) inhibit 26S proteasome-catalyzed proteolysis by sequestering lysine 48-linked polyubiquitin chains. *J Biol Chem,* **278**, 8951-8959.

Rajagopalan, K. V. (1997). Biosynthesis and processing of the moybdenum cofactors. *Biochem Soc Trans*, **25**, 757-761.

Rao, H., and Sastry, A. (2002). Recognition of specific ubiquitin conjugates is important for the proteolytic functions of the UBA domain proteins Dsk2 and Rad23. *J Biol Chem***, 277**, 11691-11695.

Richly, H., Rape, M., Braun, S., Rumpf, S., Hoege, C., and Jentsch, S. (2005). A series of ubiquitin binding factors connects CDC48/p97 to substrate multiubiquitylation and proteasomal targeting. *Cell,* **120**(1):73-84.

Rudolph, M. J., Wuebbens, M. M., Rajagopalan, K. V., and Schindelin, H. (2001). Crystal structure of molybdopterin synthase and its evolutionary relationship to ubiquitin activation. *Nat Struct Biol*, **8**, 42-46.

Ryu, K. S., Lee, K. J., Bae, S. H., Kim, B. K., Kim, K. A., and Choi, B. S. (2003). Binding surface mapping of intra- and interdomain interactions among hHR23B, ubiquitin, and polyubiquitin binding site 2 of S5a. *J Biol Chem,* **278**, 36621-36627.

Sadygov, R. G., Eng, J. K., Durr, E., Saraf, A., McDonald, W. H., MacCoss, M. J., and Yates III, J. R. (2002). Code developments to improve the efficiency of automated MS/MS spectra interpretation. *J Proteome Res*, **1**, 211-215.

Saeki, Y., Isono, E., and Toh-e, A. (2005). Preparation of ubiquitinated substrates by the PY motif-insertion method for monitoring 26S proteasome activity. *Methods in Enzymol,* **399**, 215-227.

Saeki, Y., Saito, N., Toh-e, A., and Yokosawa, H. (2002). Ubiquitin-like proteins and Rpn10 play cooperative roles in ubiquitin-dependent proteolysis. *Biochem Biophys Res Commun*, **293**, 986-992.

Salvat, C., Acquaviva, C., Scheffner, M., Robbins, I., Piechaczyk, M., and Jariel-Encontre, I. (2000). Molecular characterization of the thermosensitive E1 ubiquitin-activating enzyme cell mutant A31N-ts20. *Eur J Bioche*m, **267**, 3712-3722.

Schauber, C., Chen, L., Tongaonkar, P., Vega, I., Lambertson, D., Potts, W., and Madura, K. (1998). Rad23 links DNA repair to the ubiquitin/proteasome pathway*. Nature*, **391**, 715-718.

Schuberth, C., Richly, H., Rumpf, S., and Buchberger, A. (2004). Shp1 and Ubx2 are adaptors of Cdc48 involved in ubiquitin-dependent protein degradation. *EMBO Rep,* **5**, 818-824.

Shimada, K., Pasero, P., and Gasser, S. M. (2002). ORC and the intra-S-phase checkpoint: a threshold regulates Rad53p activation in S phase. *Genes Dev*, **16**, 3236-3252.

Stamenova, S. D., Dunn, R., Adler, A. S., and Hicke, L. (2004). The Rsp5 ubiquitin ligase binds to and ubiquitinates members of the yeast CIN85-endophilin complex, Sla1-Rvs167. *J Biol Chem,* **279**, 16017-16025.

Swanson, R., and Hochstrasser, M. (2000). A viable ubiquitin-activating enzyme mutant for evaluating ubiquitin system function in *Saccharomyces cerevisiae*. *FEBS Lett,* **447**, 193-198.

Swanson, R., Locher, M., and Hochstrasser, M. (2001). A conserved ubiquitin ligase of the nuclear envelope/endoplasmic reticulum functions in both ER-associated and Matalpha2 repressor degradation. *Genes Dev*, **15**, 2660-2674.

Tabb, D. L., McDonald, W. H., and Yates III, J. R. (2002). DTASelect and Contrast: Tools for assembling and comparing protein identifications from shotgun proteomics. *J Proteome Res*, **1**, 21-26.

van Nocker, S., Sadis, S., Rubin, D. M., Glickman, M. H., Fu, H., Coux, O., Wefes, I., Finley, D., and Vierstra, R. D. (1996). The multiubiquitin-chain-binding protein Mcb1 is a component of the 26S proteasome in *Saccharomyces cerevisiae* and plays a nonessential, substrate-specific role in protein turnover*. Mol Cell Biol,* **16,** 6020-6028.

van Nocker, S., and Vierstra, R.D. (1993). Multiubiquitin chains linked through lysine 48 are abundant in vivo and are competent intermediates in the ubiquitin proteolytic pathway. *J Biol Chem,* **268**, 24766-24773.

Verma, R., Aravind, L., Oania, R., McDonald, W. H., Yates III, J. R., Koonin, E. V., and Deshaies, R. J. (2002). Role of Rpn11 metalloprotease in deubiquitination and degradation by the 26S proteasome. *Science*, **298**, 611-615.

Verma, R., Chen, S., Feldman, R., Schieltz, D., Yates III, J. R., Dohmen, J., and Deshaies, R. J. (2000). Proteasomal proteomics: identification of nucleotide-sensitive proteasome-interacting proteins by mass spectrometric analysis of affinity purified proteasomes. *Mol Biol Cell*, **11**, 3425-3439.

Verma, R., Chi, Y., Deshaies, R. J. (1997). Ubiquitination of cell cycle regulatory proteins in yeast extract. *Methods Enzymol*, **283,** 366–376.

Verma, R., Oania, R., Graumann, J., and Deshaies, R. J. (2004). Multiubiquitin chain receptors define a layer of substrate selectivity in the ubiquitin-proteasome system. *Cell,* **118**, 99-110.

Walden, H., Podgorski, M. S., and Schulman, B. (2003). Insights into the ubiquitin transfer cascade from the structure of the activating enzyme for NEDD8. *Nature,* **422**, 330-334.

Walters, K. J., Kleijnene, M. F., Goh, A. M., Wagner, G., and Howley, P. M. (2002). Structural studies of the interaction between ubiquitin family proteins and proteasome subunit S5a. *Biochemistry,* **41**, 1767-1777.

Walters, K. J., Lech, P. J., Goh, A. M., Wang, Q., and Howley, P. M. (2003). DNA-repair protein hHR23a alters its protein structure upon binding proteasomal subunit S5a. *Proc Natl Acad Sci USA,* **100**, 12694-12699.

Washburn, M. P., Ulaszek, R., Deciu, C., Schieltz, D. M., and Yates III, J. R. (2002). Analysis of quantitative proteomic data generated via multidimensional protein identification technology. *Anal Chem*, **74**, 1650-1657.

Watkins, J. F., Sung, P., Prakash, L., and Prakash, S. (1993). The *Saccharomyces cerevisiae* DNA repair gene RAD23 encodes a nuclear protein containing a ubiquitin-like domain required for biological function. *Mol Cell Biol,* **13**, 7757-7765.

Wilkinson, C. R. M., Seeger, M., Hartmann-Petersen, R., Stone, M., Wallace, M., Semple, C., and Gordon, C. (2001). Proteins containing the UBA domain are able to bind multiubiquitin chains. *Nat Cell Biol,* **3**, 939-943.

Wolters, D. A., Washburn, M. P., and Yates III, J. R. (2001). An automated multidimensional protein identification technology for shotgun proteomics. *Anal Chem*, **73**, 5683-5690.

Xu, P., and Peng, J. (2006). Dissecting the ubiquitin pathway by mass spectrometry. *Biochim Biophys Acta,* **1764**, 1940-1947.

You, I., and Arnold, F.H. (1996). Directed evolution of subtilisin E in Bacillus subtilis to enhance total activity in aqueous dimethylformamide. *Protein Eng,* **9**, 77-83.